Accepted Manuscript

A novel class of *Plasmodial* ClpP protease inhibitors as potential antimalarial agents

Sourabh Mundra, Vandana Thakur, Angelica M. Bello, Sumit Rathore, Mohd Asad, Lianhu Wei, Jane Yang, Sai Kumar Chakka, Radhakrishnan Mahesh, Pawan Malhotra, Asif Mohmmed, Lakshmi P. Kotra

PII: S0968-0896(17)31340-8
DOI: http://dx.doi.org/10.1016/j.bmc.2017.08.049
Reference: BMC 13953

To appear in: *Bioorganic & Medicinal Chemistry*

Received Date: 30 June 2017
Revised Date: 17 August 2017
Accepted Date: 24 August 2017

Please cite this article as: Mundra, S., Thakur, V., Bello, A.M., Rathore, S., Asad, M., Wei, L., Yang, J., Kumar Chakka, S., Mahesh, R., Malhotra, P., Mohmmed, A., Kotra, L.P., A novel class of *Plasmodial* ClpP protease inhibitors as potential antimalarial agents, *Bioorganic & Medicinal Chemistry* (2017), doi: http://dx.doi.org/10.1016/j.bmc.2017.08.049

Manuscript#: BMC-2017-981 revision

A novel class of *Plasmodial* ClpP protease inhibitors as potential antimalarial agents

Sourabh Mundra,[1,3†] Vandana Thakur,[2†] Angelica M. Bello,[1,5] Sumit Rathore,[4] Mohd Asad,[2] Lianhu Wei,[1] Jane Yang,[5] Sai Kumar Chakka,[1] Radhakrishnan Mahesh,[3] Pawan Malhotra,[2] Asif Mohmmed,[2*] and Lakshmi P. Kotra[1,5*]

[1]Center for Molecular Design and Preformulations, and Toronto General Research Institute, University Health Network, Toronto, Ontario, Canada, M5G 1L7,

[2]International Centre for Genetic Engineering & Biotechnology, Aruna Asaf Ali Marg, New Delhi, India,

[3]Department of Pharmacy, Birla Institute of Technology & Science, Pilani, Rajasthan, India, 333031.

[4]Department of Biotechnology, All India Institute of Medical Sciences, New Delhi 110 029, India.

[5]Department of Pharmaceutical Sciences, Leslie Dan Faculty of Pharmacy, University of Toronto, Toronto, Ontario, Canada, M5S 3M2,

RECEIVED DATE (to be automatically inserted)

*Corresponding Authors: AM: ICGEB, Aruna Asif Ali Marg, New Delhi- 100 067, India, Email: amohd@icgeb.res.in; LPK: #5-356, TMDT/MaRS Center, 101 College Street, Toronto, Ontario, Canada M5G 1L7. Tel. (416) 581-7601, E-mail: lkotra@uhnres.utoronto.ca.
†These authors contributed equally to this work.

Abstract.

The prokaryotic ATP-dependent ClpP protease, localized in the relict plastid of malaria parasite, represents a potential drug target. In the present study, we utilized *in silico* structure-based screening and medicinal chemistry approaches to identify a novel pyrimidine series of compounds inhibiting *P. falciparum* ClpP protease activity and evaluated their antiparasitic activities. Structure-activity relationship indicated that morpholine moiety at C2, an aromatic substitution at N3 and a 4-oxo moiety on the pyrimidine are important for potent inhibition of ClpP enzyme along with antiparasiticidal activity. Compound **33** exhibited potent antiparasitic activity (EC_{50} 9.0 ± 0.2 μM), a 9-fold improvement over the antiparasitic activity of the hit molecule **6**. Treatment of blood stage *P. falciparum* cultures with compound **33** caused morphological and developmental abnormalities in the parasites; further, compound **33** treatment hindered apicoplast development indicating the targeting of apicoplast.

Key words: Malaria, ClpP protease, *in silico* docking, apicoplast, antimalarial agents.

Introduction

Malaria is a parasitic infection in humans caused primarily by *Plasmodium falciparum* and/or *P. vivax*, with a minor fraction (<10%) of the clinical cases caused by other plasmodia species. Malaria continues to burden the developing world and remains a disease of concern in the developed world despite intense efforts over the past decade to eliminate this disease. The World Health Organization (WHO) estimates that as many as 214 million cases of malaria were reported in 2015 resulting in 438,000 deaths worldwide.[1] Parasite resistance has rendered previously effective antimalarial agents ineffective in most parts of the world. Currently, artemisinin-based combination therapies (ACTs) are the standard of care for malaria. In 2009, it was confirmed that *P. falciparum* had acquired resistance to artemisinins too; therefore urgent efforts are needed to combat these drug-resistant parasites.[2,3] A recent report that surveyed a defined region in the endemic areas of India estimated that adult and child mortalities due to malaria are vastly underreported, and that the estimates of the WHO are at least 10 times less than may occur in the field at the time of the survey, suggesting a massive gap between the WHO estimates and the reality in endemic areas.[4] These combined factors underscore the need for new measures in the prevention and treatment of malaria.

Variants of known drug classes are no longer acceptable because there is a higher chance for the development of cross-resistance to these drugs. The campaign for malaria treatments stresses the need for new and different classes of antimalarial drugs that will be effective in treating current drug resistance parasites,[5] and in accordance with this, the efforts in the past year have shifted towards developing novel classes of antimalarial drugs. Another attractive approach would be to develop drugs directed against novel targets that have not yet been fully exploited for therapeutic use.

ATPase dependent protease machineries such as eukaryotic 26S proteasome and the prokaryotic caseinolytic proteases (ClpP) systems are large protein degradation complexes that play an essential role in cell cycle regulation.[6,7] The *P. falciparum* genome also harbors cyanobacterial ClpP

protease, PfClpP, and its putative ATPase partner. The ATPases assemble into large multi-subunit complexes with the ClpP proteases and act as chaperons to unfold the substrate proteins which subsequently get degraded by the protease component. The PfClpP is localized in the apicoplast as determined by the GFP targeting approach, immunoelectron microscopy and by immunofluorescence assays.[8] The apicoplast is a reduced cyanobacterial plastid in the parasite; the metabolic pathways in the mitochondrion and the apicoplast, two parasite organelles of prokaryotic origin, may represent suitable drug targets in the parasite. Apicoplast plays an important role in biosynthesis of haeme, isopentenyl diphosphate and fatty-acids,[9] thus the apicoplast is considered to be important for parasite survival. Indeed, antibacterial agents such as ciprofloxacin, rifampicin and thiostrepton that target DNA replication, transcription and translation of the apicoplast respectively, have been also shown to kill the parasite.[10,11,12,13]

P. falciparum contains two ClpP proteases, a PfClpP (gene ID: PF3D7_0307400), and one PfClpR (gene ID PF3D7_1436800); the parasite also contains four Clp ATPases (PfClpB1, PfClpB2, PfClpC, and PfClpM), all these proteins are expressed in blood stages of the parasite.[8,14] The ClpP and ClpR proteases are shown to be localized in parasite apicoplast.[8,14] Earlier, we also screened cell-permeable β-lactones that bind at the active site of prokaryotic ClpP, and identified compounds that inhibit the development of apicoplast leading to parasiticidal activities.[8] The crystal structure of PfClpP shows the presence of the conserved active site triad of serine proteases (PDB: 2F6I),[15] and it forms compacted tetra-decamer; such oligomerization was also observed in the case of ClpP proteases from *Streptococcus pneumoniae* and *Mycobacterium tuberculosis*.[14] In the present study, we conducted *in silico* screening of chemical compound libraries using the active site of PfClpP to identify a small set of hit compounds; novel series of compounds were designed and synthesized based upon the structures of the hit compounds. *In vitro* screening of selected compounds using enzyme activity assays and parasite growth inhibition assays identified potential lead compound

targeting PfClpP with antimalarial activities.

Results.

The structures of ClpP proteases from different organisms have shown two distinct conformational states. An extended state three-dimensional structure is gleaned from the ClpP protease structures of *E. coli*, *Homo sapiens*, and *Helicobacter pylori*. In the extended state, the catalytic triad is generally organized and pre-positioned for a catalytic reaction. The second state, a compact state is observed in the three-dimensional structures of ClpP protease from *S. pneumonia*, *P. falciparum* and *M. tuberculosis*, which is an inactive state. Three-dimensional structure of PfClpP protease in its extended state is not available. The extended state of *E. coli* crystal structure (RCSB code: 2FZS)[16] was used as a template to model the *P. falciparum* ClpP protease and was used for *in silico* screening. *In silico* screening was focused on the S1 and S1'pockets in the active site of ClpP protease (Figure 1), and it was carried out using commercially available compounds library containing 450,000 small molecule structures; this study ultimately led to the identification of 13 hits (**1-13**) meeting all the screening criteria including their potential for further medicinal chemistry (Table 1).

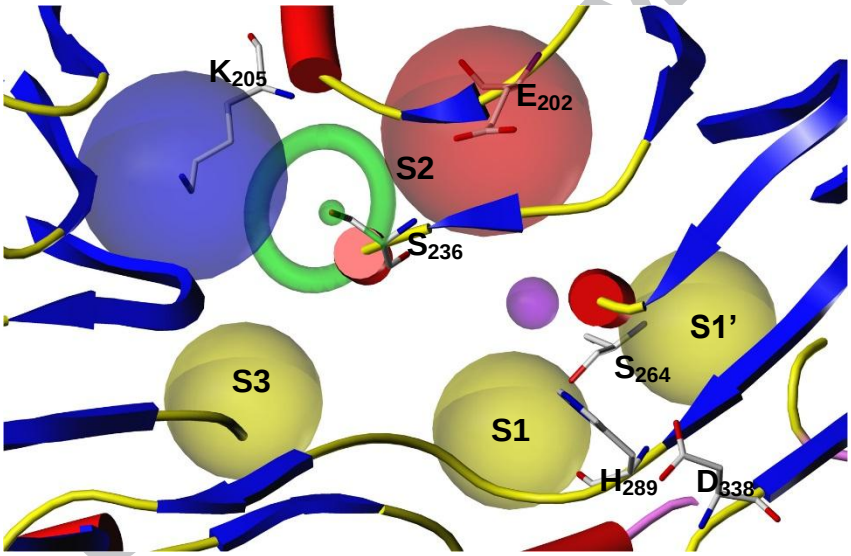

Figure 1. Illustration of the features defined in the active site of *Pf* ClpP protease. Protein sequence is shown as a cartoon model, and the amino acid residues are shown in capped-stick representation (C: white, O: red, N: blue). Active site features are depicted over the active site of the enzyme using the following color-coding: hydrophobic feature: yellow sphere; anionic center: red sphere; cationic center: blue sphere; magenta sphere: hydrogen bond acceptor corresponding to S_{264}; green ring: hydrogen bond donor. S1', S1, S2, S3 indicate the protein binding site positions of *Pf* ClpP.

These 13 hit compounds, **1-13** were evaluated for their

potential to inhibit PfClpP protease followed by their antiparasitic activity. Five compounds **1, 2, 4, 6**, and **11** exhibited appreciable inhibition of PfClpP protease activity with inhibition constants (IC_{50}) lower than 100 µM. These five compounds were then evaluated for their antiparasitic activities against *P. falciparum*. Compounds **1**, **6** and **11** inhibited parasite growth with inhibition constants (IC_{50}) in the range of 25-75 µM. Upon comparison of the structures of these three active compounds, and the ease of synthetic feasibility to functionalize the core structural elements, the common pyrimidine core of compounds **6** and **11** was further pursued (Figure 2).

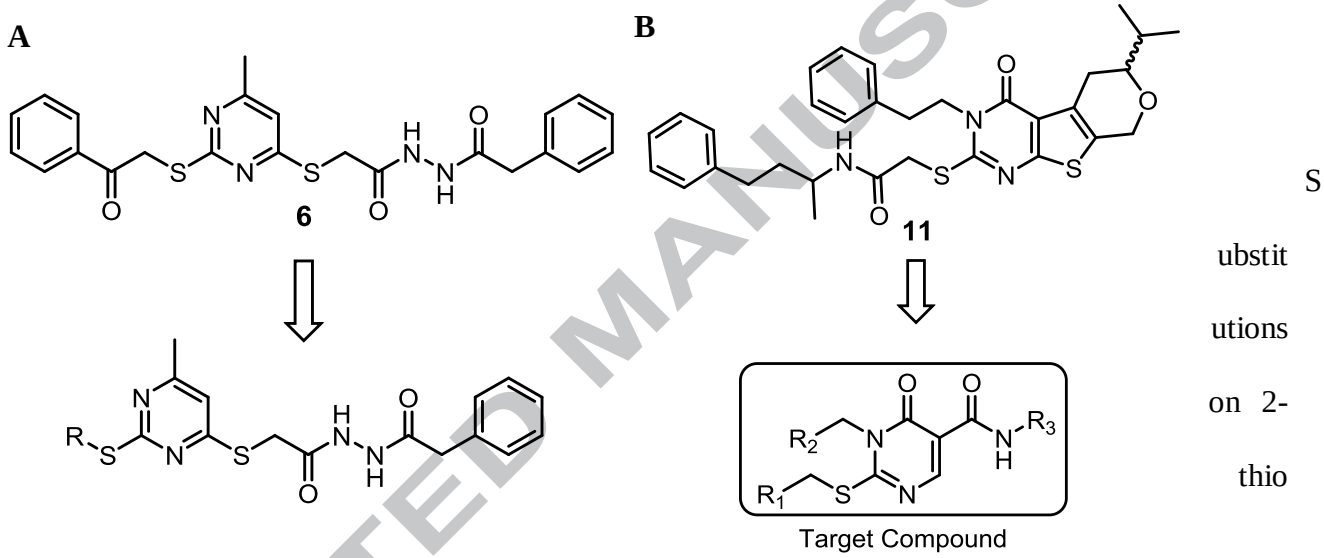

Figure 2. Design of analogs based on compounds **6** (panel A) and **11** (panel B).

Substitutions on 2-thiopyrimidin-2-thione, including *p*-methoxyphenyl, *p*-diethylaminophenyl, morpholinyl and 4-benzonitrile moieties, were synthesized in order to investigate structure-activity relationship (Scheme 1). Synthesis of compounds **22-26** was initiated starting from 6-methyl-2-thio-2-pyrimidinone (**14**) (Scheme 1A). Alkylation of compound **14** using an appropriate halide in the presence of potassium carbonate in DMF yielded the thioethers **15A-15E**. Compounds **15A-15E** were subjected to chlorination using phosphorous oxychloride to obtain the corresponding chlorothioethers **16A-16E**, which were used as intermediates *en route* to the target compounds **22-26** (Scheme 1B). Thus phenyl methylacetate (**17**)

was treated with hydrazine hydrate to obtain the hydrazine **18**, which was further treated with chloroacetyl chloride to obtain compound **19** in 66% yield. Compound **19** was then treated with potassium thioacetate, followed by saponification to yield compound **21** in approximately 70% yield for each transformation. Compound **21** was then coupled to compounds **16A-16E** by the substitution of the chloro moiety to yield compounds **22-26**, respectively.

Scheme 1. Synthesis of compounds **22-26**. Reagents and conditions: (i) **A-E** halides, K_2CO_3, DMF, 16 h, rt; (ii) $POCl_3$, 70 °C, 1 h; (iii) $NH_2NH_2 \cdot H_2O$, MeOH, 16 h, rt; (iv) chloroacetyl chloride, DIPEA, CH_2Cl_2, -10 °C to rt, 30 min; (v) AcS^-K^+, EtOH, rt; (vi) K_2CO_3, MeOH, rt, 1 h; (vii) compounds **16A-16E**, Et_3N, AcCN.

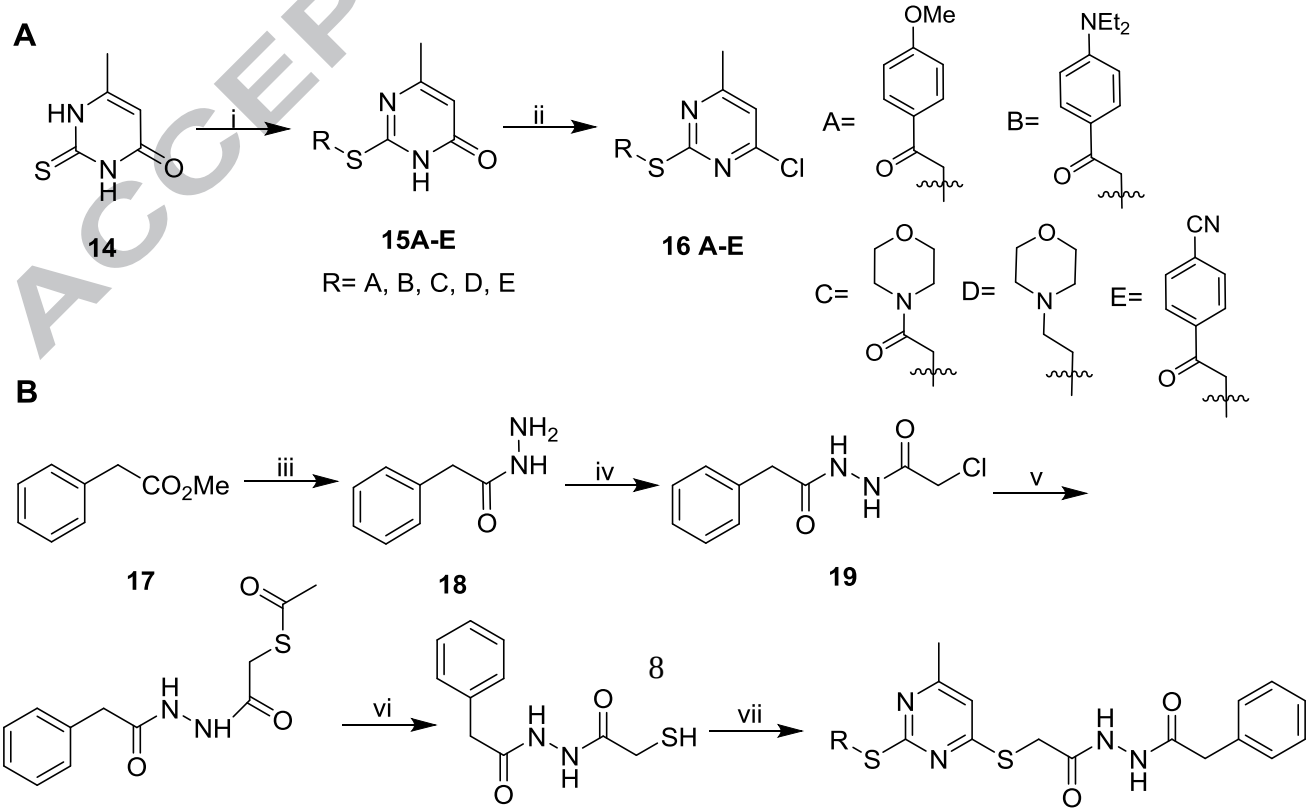

Compounds **30-38**, designer compounds based on the core structure derived from compound **11** (Figure 2B) were synthesized using the chemical synthesis illustrated in Scheme 2. Benzyl thiourea (**27**) and diethyl (ethoxymethylene)malonate were cyclized to yield 2-thio-3-benzyl uracil derivative **28** in 55% yield. Compound **28** was transformed into the phenylpropyl amine derivative **29**; compound **29** was alkylated using appropriate alkyl halides in the presence of potassium carbonate to yield compounds **30**-**38** in 30-50% yield. Additional derivatives bearing a morpholine moiety such as **40**-**42** and **44** were synthesized from 2-mercapto-5-carboxyethyl uracil (**39**). Alkylation of the thio moiety with acetohydrazide or bromoethylmorpholine gave compounds **40** and **41**, respectively (Scheme 3). Alkylation of N3 position on **41** with bromoacetophenone yielded compound **42**. Hydrolysis of ethyl ester **42** led to the cyclized bicyclic thiazine derivative **43**, and did not provide the intended product of monocyclic 5-carboxy-2,3-substituted pyrimidine derivative. Thus, compound **41** was then derivatized at C5 position introducing phenylpropylamine moiety to yield compound **44** in 60% yield. It was also evident that introduction of substitutions onto 2-thiouracil at 2, 3 and 5 positions is more efficient via thiourea-malonate condensation pathway (Scheme 2), and introduction of acetophenyl moiety makes the compounds susceptible to cyclization (such as **42** to **43**).

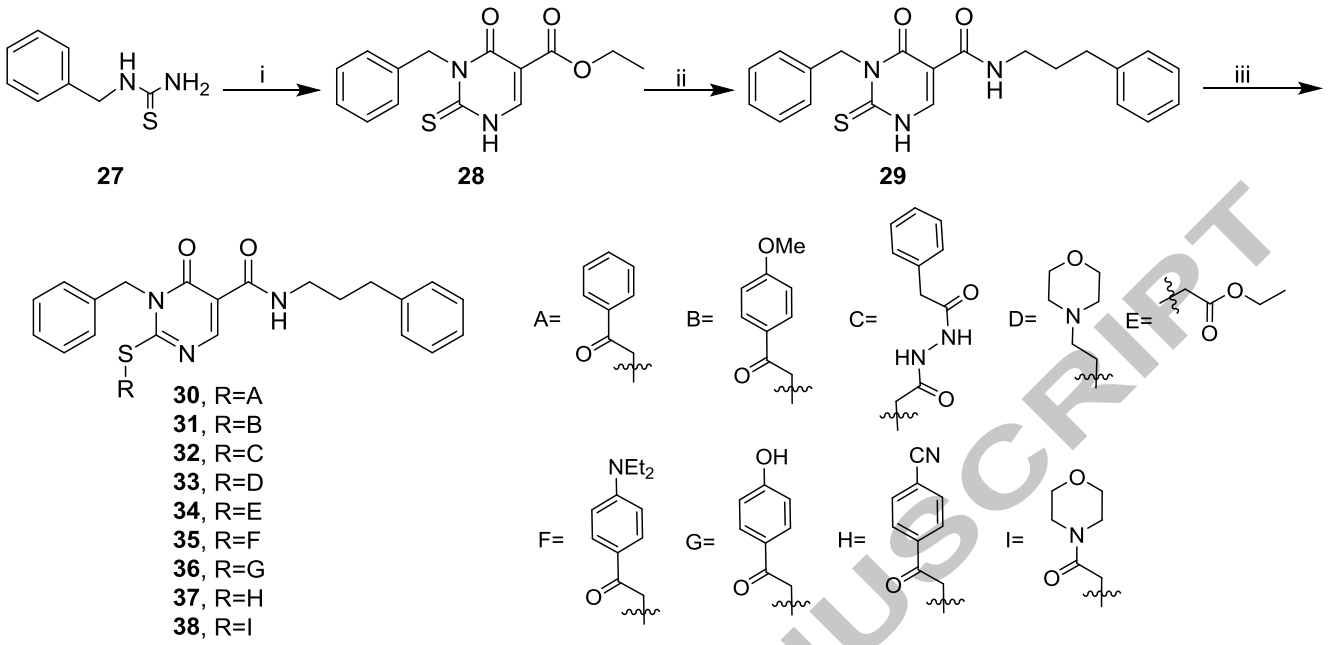

Scheme 2. Synthesis of compounds **30-38**. Reagents and conditions: (i) Diethyl (ethoxymethylene)malonate, K_2CO_3, DMF, 120 ºC, 1 h; (ii) 3-Phenyl-1-propylamine, trimethyl aluminum, 16 h, 0 °C to rt; (iii) A-I halides, K_2CO_3, DMF, 16 h, rt.

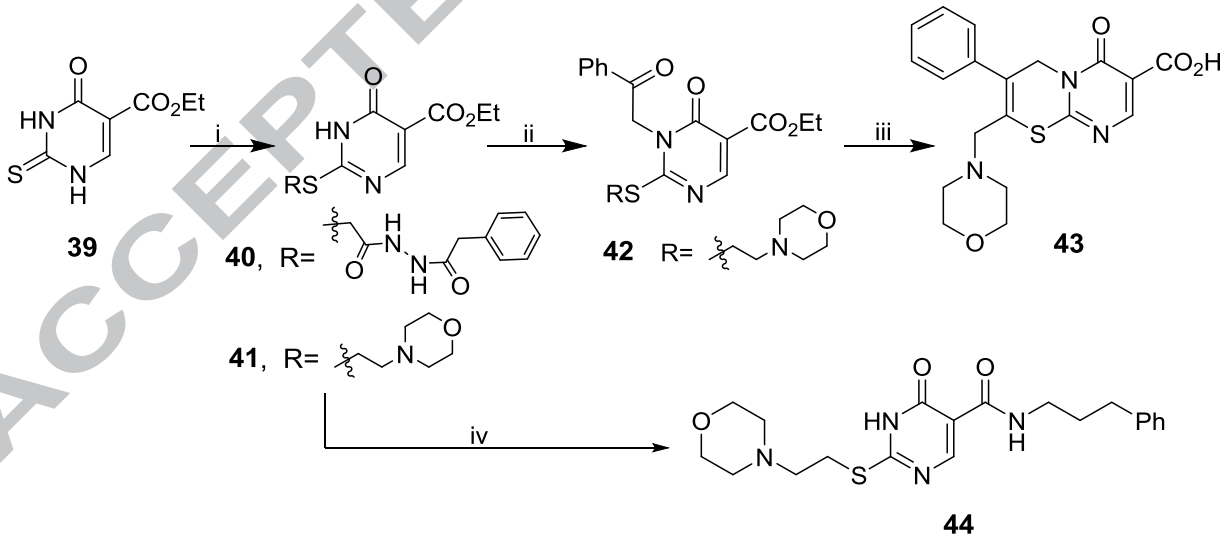

Scheme 3. Synthesis of compounds **40-44**. Reagents and conditions: (i) 2-Chloro-*N*'-(2-phenylacetyl)acetohydrazide or 4-(2-bromoethyl)morpholine, K_2CO_3, acetone, 16 h, rt; (ii) 2-Chloroacetophenone, K_2CO_3, acetone, 16 h, rt; (iii), LiOH in THF/MeOH (3:1) 16 h, rt; (iv) 3-Phenylpropylamine, trimethyl aluminium, 16 h, 0 °C- rt.

Identification of specific PfClpP inhibitors with parasiticidal efficacies. All synthesized compounds were evaluated for their inhibitory activities against recombinant PfClpP protease. Compounds that exhibited PfClpP enzyme inhibition (IC_{50}) at less than 100 μM concentration were then evaluated for their antiparasitic activities. Compounds **1**, **2**, **4**, **6** and **11**, which were the hits from the *in silico* screening showed promising enzyme inhibition with inhibition constants (IC_{50}) in the range of 22-92 μM and the corresponding apparent K_i in the range of 9-37 μM. These compounds were subsequently evaluated for their antiparasitic activities; compounds **1, 6** and **11** showed moderate inhibition with IC_{50} ranging from 25-75 μM. These three compounds were also tested for cytotoxicity in HeLa cell line, and all three compounds showed IC_{50} > 5 mM.

Compounds **22-26**, which are based on the core structure **6** inhibited the PfClpP protease activity with moderate potency with IC_{50} in the range of 28-35 μM. Compounds **22-26** inhibited *P. falciparum* parasite cultures with IC_{50}s in the range of 11.8-17.3 μM. Compounds **30-32**, **40**, **42** and **44** showed moderate to good inhibition of PfClpP protease activity, with IC_{50}s in the range of 10-72 μM. Compound **30** is the most active compound in this group of inhibitors, with an IC_{50} of 24±8 μM, and the apparent K_i = 10±3 μM (Table 1). Compounds **41** and **43** did not exhibit appreciable inhibition of PfClpP protease, upto 100 μM concentration. Compound **33** exhibited the most potent inhibitory activity of all tested compounds against PfClpP protease, with an IC_{50} of 10.5 ± 0.2 μM (apparent K_i = 2.3 ±0.2 μM). Compounds **34-38** exhibited either weak or no inhibition of PfClpP protease activity; specifically compounds **34, 36** and **38** inhibited the protease activity at concentrations (IC_{50}) in the range of 45-58 μM. Compounds **35** and **37** did not inhibit the protease activity upto 100 μM concentration.

Table 1. ClpP Enzyme inhibition and parasite growth assay.

Compound	Structure	PfClpP Protease Inhibition		*P. falciparum* inhibition
		IC_{50} ± SE (μM)	K_i (μM)	IC_{50} ± SE (μM)
1	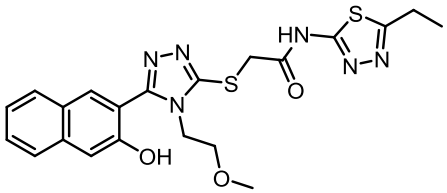	30.0 ± 4.0	12.1 ± 0.2	27.0 ± 2.0
2	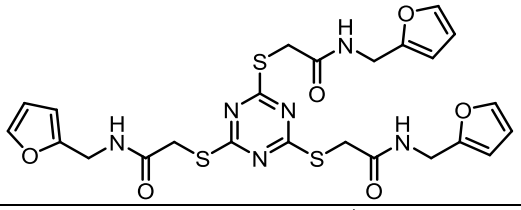	92.0 ± 105.0	38.0 ± 43.0	NA
3	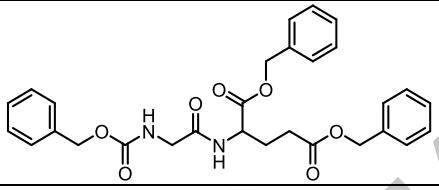	>100.0	NA	NA
4	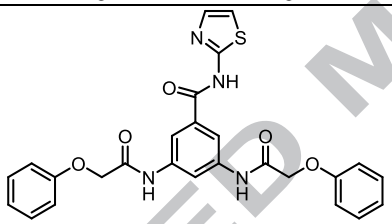	88.0 ± 31.0	36.0 ±13.0	NA
5	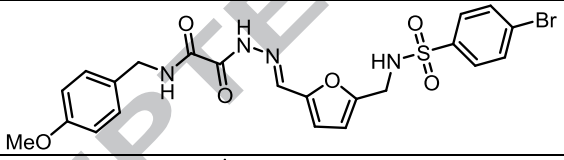	>100.0	NA	NA
6	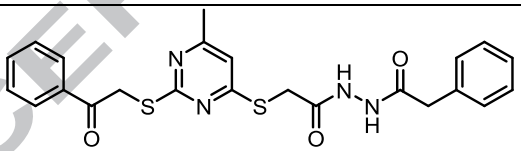	26.0 ± 6.0	11.0 ± 2.0	75.0 ± 9.0
7	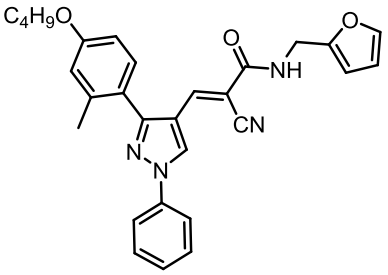	>100.0	NA	NA

8	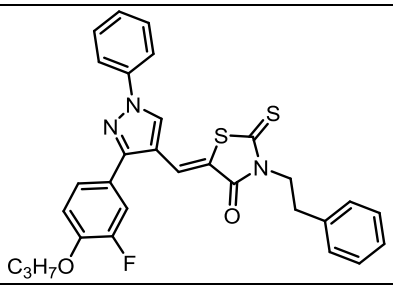	>100.0	NA	NA
9	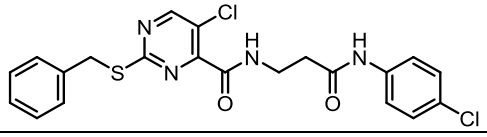	>100.0	NA	NA
10	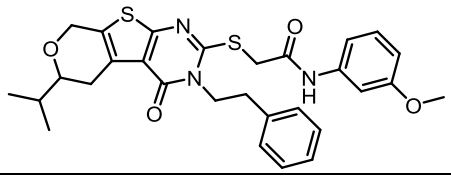	>100.0	NA	NA
11	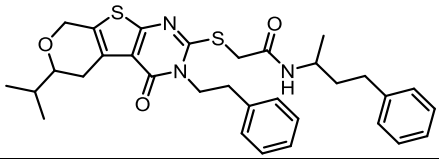	23.0 ± 10.0	9.0 ± 4.0	25.0 ± 4.0
12	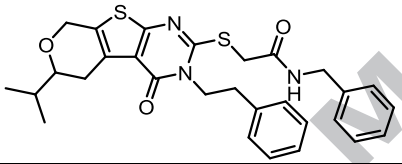	>100.0	NA	NA
13	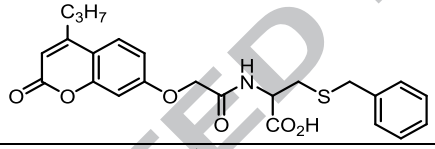	>100.0	NA	NA
22	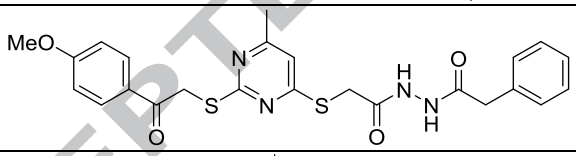	34.7 ± 0.5	14.2 ± 0.2	11.80 ± 0.03
23	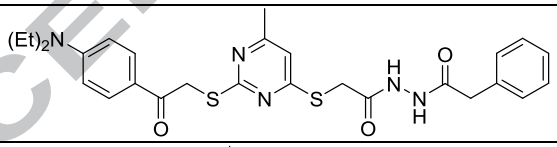	28.3 ± 0.4	11.6 ±0.2	12.14±0.03
24	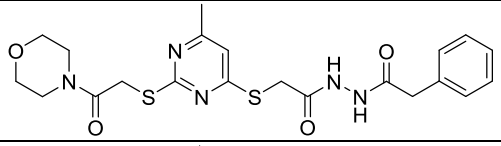	28.8 ± 0.4	11.8 ± 0.2	17.3 ± 0.1
25	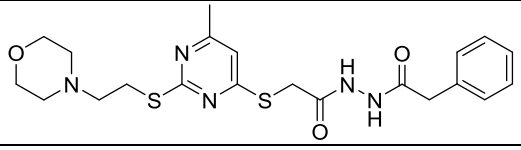	30.3± 0.1	12.3 ± 0.1	14.4 ± 0.1

26	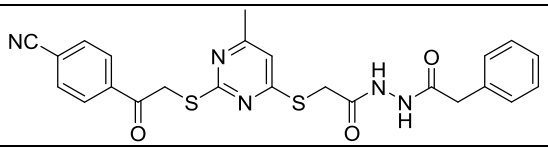	37.4± 0.2	15.3 ±0.1	12.4 ±0.1
30	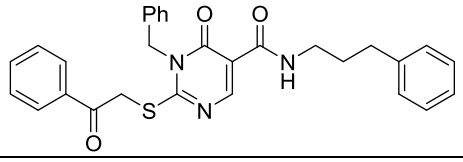	24.0 ± 8.0	10.0 ± 3.0	20.0 ± 2.0
31	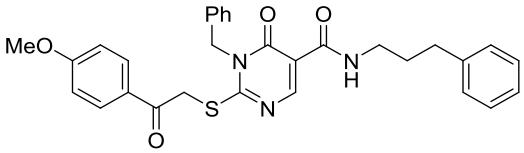	45.0 ± 13.0	18.0 ± 5.0	2.4 ± 1.5
32	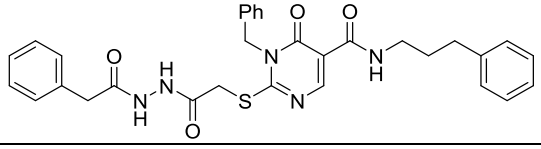	72.6 ± 44.4	29.5 ± 18.0	NA
33	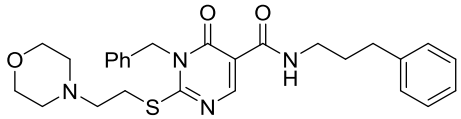	10.5± 0.2	2.3 ± 0.2	9.0 ± 0.2
34	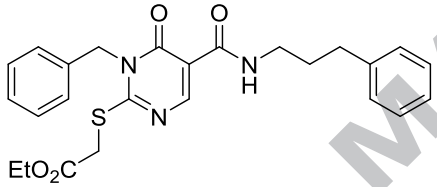	58.3 ± 0.1	23.8 ± 0.1	15.9±0.1
35	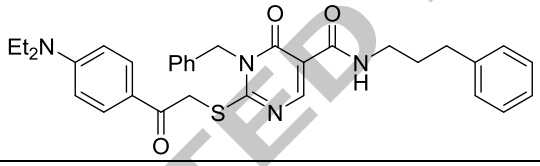	>100.0	NA	9.2 ± 0.1
36	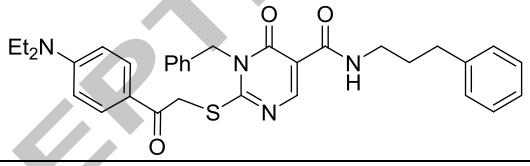	53.0 ± 0.1	21.6 ± 0.1	9.2 ±0.1
37	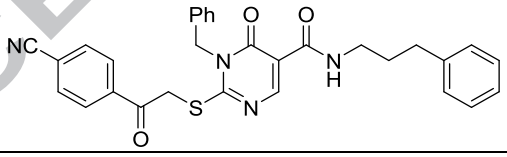	>100.0	NA	13.7 ± 0.1
38	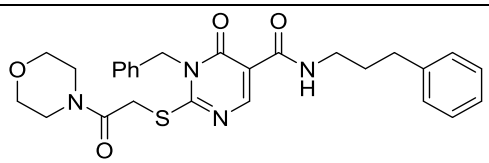	46.0 ± 0.7	18.8 ± 0.3	11.7 ± 0.1
40	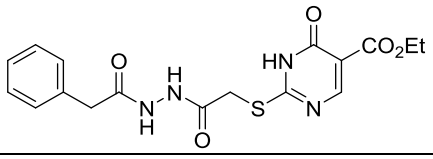	42.0 ± 8.0	17.0 ± 3.0	82.5 ± 0.5

41	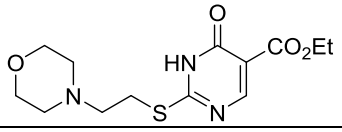	>100.0	NA	NA
42	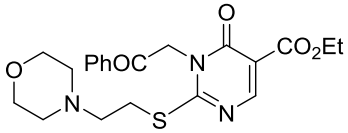	40.0 ± 12.0	16.0 ± 5.0	19.0 ± 2.0
43	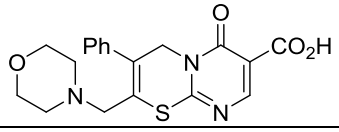	>100.0	NA	11.0 ± 2.0
44	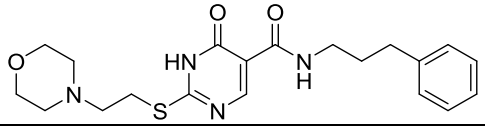	44.0 ± 7.0	18.0 ± 3.0	22.0 ± 0.5

Compounds **30-33**, **40**, **42** and **44**, which are the active compounds against the protease activity, were then evaluated for their inhibition of *P. falciparum* growth in the culture. Compound **30** inhibited *P. falciparum* growth at a concentration (IC_{50}) of 20.0±2.0 μM, as expected based on its activity against ClpP protease. Compound **31** inhibited *P. falciparum* cultures at a concentration (IC_{50}) of 2.4 ± 1.5 μM, about 20-fold higher potency than the IC_{50} for the inhibition of PfClpP protease. Compound **32** did not inhibit *P. falciparum* growth even at 100 μM concentration. Compound **33** inhibited *P. falciparum* at a concentration of 9.0±0.2 μM, and compounds **34-38** similarly inhibited *P. falciparum* growth with IC_{50}s in the range of 9.2-15.9 μM, somewhat higher potency than that for the inhibition of the target enzyme. Compound **40** inhibited the parasite growth with moderate potency of IC_{50} at 82.5±0.5 μM. Compounds **42** and **44** inhibited the parasite growth at 19.0±1.5 μM and 21.9±0.5 μM, respectively, which are about 2-fold higher potency than their corresponding *in vitro* PfClpP protease activity inhibition (Table 1).

Compound **33** was further studied for cytotoxicity using HeLa cell line. This compound exhibited an IC_{50} >5 mM in this cell line indicating high selectivity for its parasiticidal effects.

Effect of ClpP inhibitors on plasmodial parasite development. We investigated the effect of one of

the most active compounds in the series, compound **33**, on the morphology and development of *P. falciparum* during the asexual stages (Figure 3). The ring stage parasites were treated with the protease inhibitor **33** or no treatment. The parasites developed from ring stage to trophozoite stage and subsequently developed into the schizont stage in the first 48 h, when there was no inhibitor present in the growth culture; the merozoites also invaded fresh erythrocytes and completed the second cycle during 48-96 h of incubation. The compound **33**-treated parasites were developmentally arrested at the transition from early to late stage schizont. The abnormal parasites in cultures were not able to develop into mature schizonts, and were seen as abnormal parasites even at 60 hpi (Figure 3). These phenotypes in second cell-cycle after treatment with compound **33** are similar to those seen in parasites treated with other inhibitors known to be targeting apicoplast targets.[17,18]

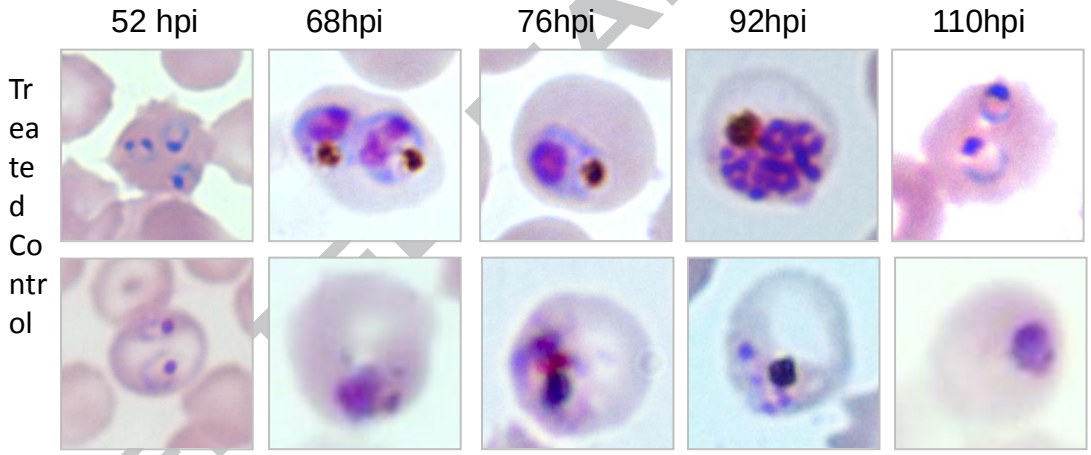

Figure 3. Effect of compound **33** on development and morphology of *P. falciparum* parasites. Growth of trophozoite stage parasite and development of schizonts was inhibited in **33** treated parasite cultures.

Effect of PfClpP inhibitors on apicoplast development. Since ClpP is an apicoplast protease, the effect of inhibitor **33** was assessed on growth and development of the apicoplast, we utilized the transgenic parasite line expressing nuclear-encoded GFP fusion protein, which is targeted to the apicoplast. The growth and development of the apicoplast during the first cell cycle in the parasites treated with **33** at 10 μM concentration were indistinguishable from that of untreated parasite; the

apicoplast showed elongated and branched pattern in the early schizont-stage parasites and divided normally (Figure 4). However, during the second cell cycle the growth and development of apicoplast was severely affected by the treatment with compound **33**. In the trophozoite stages of the second cell cycle, the apicoplast was seen as spherical structure in the treated cultures, as in case of the control set; however, the apicoplast was not able to grow and divide during the schizogony in the treated cultures. In the early schizont-stage (72 h after the drug treatment) and the late schizont-stage parasites (90–96 h after drug treatment), the apicoplast appeared as a round stump-like structure without any branching and segregation. However, the nuclear divisions in these parasites proceeded normally and at 96 h the multinucleate parasites were observed with a single apicoplast (Figure 4). Overall, the compound **33**, a specific inhibitor of PfClpP, showed targeted effect on apicoplast development and segregation during the second cell-cycle after treatment.

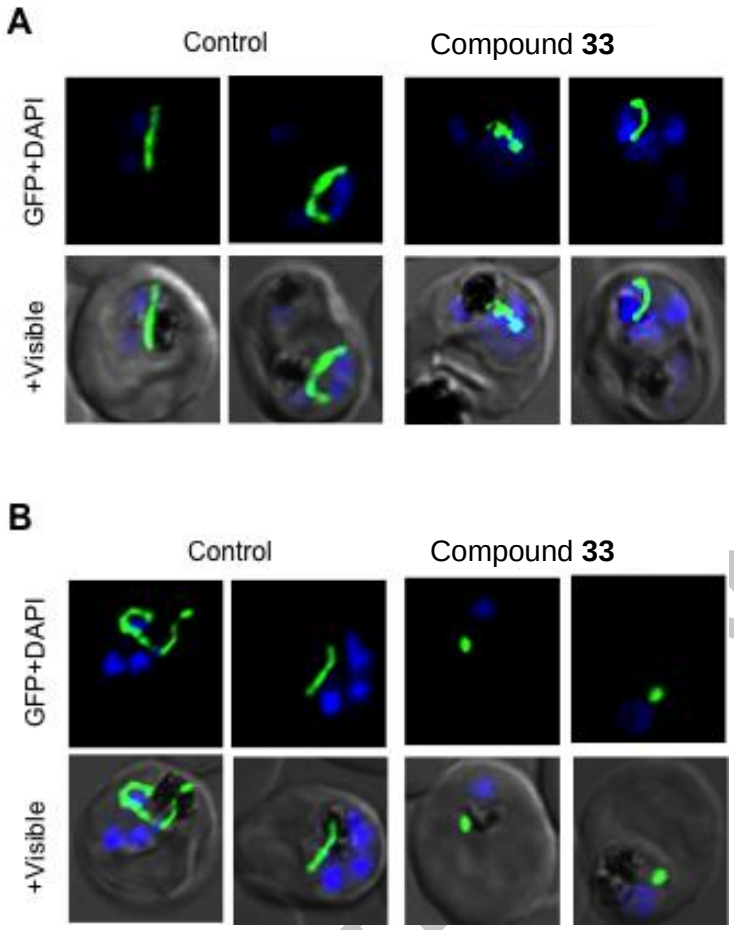

Figure 4. Effect of compound **33** on apicoplast development in *P. falciparum*. Fluorescence microscopic images of D10-ACP-GFP parasite showing development of apicoplast at 36hpi (A) and 72hpi (B) in parasite cultures treated with **33** at IC_{50} concentration. The apicoplast development in treated parasite was severely inhibited in treated cultures.

Discussion.

The apicoplast is a specialized organelle in the malaria parasite with prokaryotic origin. Several metabolic pathways in this organelle are unique to the parasite as compared to the host and thus these

pathways are good targets to design new antimalarials. The *P. falciparum* ClpP serine protease (PfClpP), homologue of a cyanobacterial ClpP, is one such potential drug target. The ClpP is localized in the apicoplast and plays an essential role in the apicoplast growth and development.[8] Parasite proteases have been considered as potential drug targets for malaria as they play crucial roles in different metabolic pathways and can be inhibited by specific inhibitors.[19,20] The crystal structure of PfClpP (PDB ID: 2F6I) shows the presence of the conserved active site triad of serine proteases; this protease forms a compact, inactive tetradecamer as in the case of ClpP proteases from *Streptococcus pneumoniae* and *Mycobacterium tuberculosis*.[14] Three dimensional structure of "extended" PfClpP protease in its active state is not resolved. Therefore, we used the extended state of *E. coli* crystal structure (PBD code: 2FZS) as a template to model the extended state of *P. falciparum* ClpP. This energy minimized 3D extended state PfClpP model was used for *in silico* high throughput screening of large compound libraries to identify potential inhibitors. Initial *in silico* screening combined with activity assay based screening identified five compounds, **1**, **2**, **4**, **6** and **11**, showed inhibitory activity on PfClpP enzyme and also showed promising effect on parasite growth with moderate potency (IC_{50} in the range of 5 μM) (Table 1). Other compounds did not show appreciable activities against either ClpP protease or the parasite growth.

Based on the structures of compound **6** and **11**, two series of substituted pyrimidine derivatives were synthesized (Figure 2). Initially, we examined the role of C2 substitution on the pyrimidine moiety using the first set of compounds **22-26**. The substitutions included morpholine moiety and substituted phenyl moieties. None of these compounds exhibited superior inhibition of ClpP protease when compared to compound **6**, but were almost equipotent. Based on this small set of compounds, it was concluded that *p*-substituted benzyl moieties at C2 position via a thioether linker (compounds **22**, **23** and **26**) did not contribute towards any changes in the activities, as was the case for the morpholine substitution (compounds **24** and **25**).

The second set of compounds, **30-38** and **40-44** were evaluated using the primary and secondary assays, i.e. ClpP protease assay and the *P. falciparum* culture assay, respectively. Inhibition of ClpP protease activities and the corresponding antiparasitic activities of compounds **30-33** indicated that the morpholinoethylthio substitution at C2 position rendered good activity to compound **33**, and the aromatic substitutions at C2 on compounds **30-32** only offered moderate to poor potency. Compound **34**, with a C2-ethylacetyl substitution, and compounds **35-37** and **40**, with C2-aromatic substitutions were only weak or inactive compounds against ClpP protease. Compounds **42** and **44**, both carrying a morpholino moiety at C2 but no bulky substitution either at N3 or C5 (**42** vs **44**), exhibited only moderate inhibition of ClpP protease activities (IC_{50} 40±12 and 44±7 μM, respectively), and moderate antiplasmodial activities. Compounds **38**, **41** and **43** did not show any inhibition of ClpP protease, at upto 100 μM concentration, despite the presence of morpholino moiety on the C2 side chain. Close inspection of the structures of compounds **33**, **38** and other morpholine carrying sidechains at C2 indicate that the presence of a tertiary amide involving morpholine compromises the potency against the inhibition of ClpP protease. The length of the side chain at C2 is optimal at 3 atoms (i.e. thioethyl) in the most active compounds. C4-Methyl substitution as in compounds **22-26** did not provide any advantage over 4-ketone (compounds **30-38** and **40-44**) on the pyrimidine moiety; in addition benzyl substitution at N3 provided important hydrophobic character with improved potency, somewhat supporting the core structure based on compound **11** (Figure 2B).

Upon comparing the C6 substitutions on compounds **22-26**, and C5 substitutions on compounds **30-38** and **40-44**, a general trend towards hydrophobic groups substituted at C5 position may enhance activity. Although this needs to be investigated further, C6 substitution alone did not help improve the biological activities, but two substitutions at C5 (ethoxycarbonyl and phenylpropylaminocarbonyl moieties) helped maintain the antiparasitic activities and is not a prohibitive substitution. Above observations are summarized in Figure 5, illustrating the importance of each substitution on the

pyrimidine moiety (Figure 5).

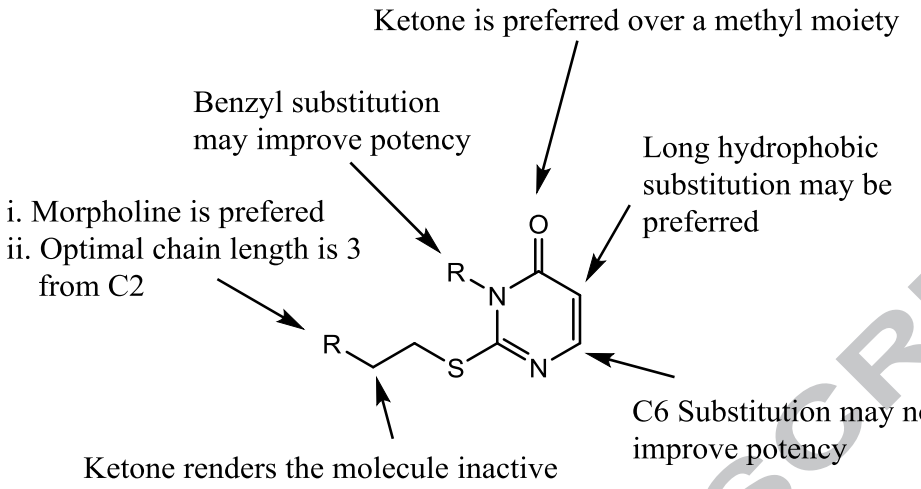

Figure 5. General structure-activity observations based on the pyrimidine core structure, and the derivatives of **6** and **11**.

Among the active compounds, most effective compound **33** was selected to study detailed effect on parasite growth and development (Figures 3 and 4). A number of apicoplast targeting drugs are shown to severely affect ability of the apicoplast to grow and segregate in the subsequent cycle leading to death of the parasite.[21,22,23,24,25] Since ClpP is an apicoplast protein, its inhibitors are expected to specifically effect the development of apicoplast in the subsequent cycle of the parasites. Our data show that inhibition of the PfClpP by selected inhibitor **33**, inhibited the growth and segregation of apicoplast in the subsequent cell cycle after treatment, which hampered the development of schizonts in that cycle, ultimately causing parasite death (Figure 3).

Currently, the most effective compounds utilized in antimalarial therapy programs belong to single class of compounds, the artemisinins; however, resistance is already emerging against artemisinins. To avoid generation of drug-resistance and for effective malaria cure, combinations therapies are developed; however, most of these combination therapies utilize artemisinin along with other anti-malarial drugs for which resistance in parasite is already reported. Therefore, there is a need to develop new drugs, which can be utilized in combination therapy with artemisinins. Understanding

the mechanisms by which a new drug kills the parasite may help to assess its potential in combination therapies. It has been suggested that slow acting, apicoplast targeting drugs can be effectively used as combination therapy with fast acting artemisinin based drugs; further, these drugs in combination with artemisinin may even slow the spread of artemisinin resistance.[26,27] Overall our studies using *in silico* screening and structure activity relationship analysis led to identification of novel pyrimidine class of compounds targeting PfClpP protease. We reveal that these molecules specifically target the apicoplast in the *P. falciparum* parasite and inhibit parasite growth, these compounds can be developed further to design new antimalarials which can be used in combination therapy strategy.

Experimental Section.

Molecular modeling and docking procedures: Three-dimensional structure of the tetra-decamer form of *P. falciparum* ClpP protease was generated based on the X-ray crystal structure of *E. coli* ClpP protease. Then the structure was subjected to energy minimization using Amber version 11.0 suite molecular simulation package.[28] An all-atom force field and the default atomic charges for the residues were used as implemented in Amber software package (ff03 force field). The molecule was immersed in a rectangular TIP3P water box that is at least 9 Å from the surface of the protein before performing energy minimization. During energy minimization, non-bonded interactions were computed for up to a distance of 12.0 Å. The molecular systems were first energy-minimized using steepest decent method for 50 cycles and then using conjugate gradient method up to 20,000 cycles. Then the energy minimized 3D extended PfClpP model was used for in silico high throughput screening.

The *in silico* screening focused on the active site of PfClpP protease; S1 and S1'pockets in the active site of ClpP protease are hydrophobic, and are surrounded by I_{237}, M_{265}, V_{268}, P_{291}, L_{316}, and L_{320}. S3 pocket is also hydrophobic, which is ensconced by the side chains of L_{241}, I_{237}, L_{312}, and L_{261} (spheres in yellow, Figure 1). Thus, three hydrophobic centers were defined representing S1, S3, and

S1 pockets' surface properties. A hydrogen bond donor feature is defined on the side chain of S_{236} (green ring in Figure 1), and a hydrogen bond acceptor feature was defined using the side chain of S_{264} (sphere in magenta, Figure 1), which is the catalytic residue for proteolysis. An anionic center representing the side chain of K_{205}, a cationic center representing the side chain of E_{202} were defined as the active site features for the *in silico* screening. A total of seven active site features were defined and were used as a template for UNITY database search. The Unity3D flexible search was performed using the following rules for the filtering of the small molecules: (1) match the hydrophobic features S1 and S3, and the hydrogen bond acceptor feature; (2) match at least one of the remaining four features. Commercial chemical libraries from Asinex, Otava, and Pharmeks containing a total of over 450,000 compounds, customized in-house, were used for this screening and total 1,768 hits from the UNITY search were obtained. There are 251 hits out of Asinex Platinum library, 257 hits out of Asinex Gold library, 58 hits out of Asinex Elite library, 575 hits from Pharmeks library, 278 hits from Otava in-house library, and 349 hits from Otava backorder library. These were then docked to PfClpP protease active site using GOLD program from CCDC (http://www.ccdc.cam.ac.uk). In the docking procedure, all the active site residues were kept rigid. Gold scoring function was used to choose the top ranking hits and all ligands were used 40 GA runs. The top 225 hits (GOLD fitness scores cut-off is 73) was chosen for the next round of manual selection, which were narrowed down to 13 compounds based on their chemical structures, and potential to synthesize analogs for optimization.

Chemistry. All solvents and chemical reagents were obtained from commercial sources. All anhydrous reactions were performed under a nitrogen atmosphere; anhydrous solvents were prepared following standard procedures. Reaction progress was monitored by TLC plates (Silica gel-60 F_{254}). Chromatographic purifications were performed using silica gel (60 Å, 70-230 mesh). The purchased library compounds were characterized by ^{1}H NMR, UV and mass spectral analyses. Purity data for the synthesized compounds were obtained using two independent methods using a Waters® HPLC system

equipped with a photodiode array detector employing reverse phase chromatography (XBridge analytical C_{18} column, 4.6x150 mm^2, 5 μm) (determined to be >95%, supplemental information). Mass spectra for all compounds were recorded using Waters® MS3100 mass spectrometer in the ESI +ve mode. NMR spectra for all compounds were recorded on a Bruker NMR spectrometer (400 MHz for ^1H and 101 MHz for ^{13}C nuclei). Chemical shifts are reported in δ ppm using tetramethylsilane (TMS) as a reference.

***N*-(5-Ethyl-1,3,4-thiadiazol-2-yl)-2-((5-(3-hydroxynaphthalen-2-yl)-4-(2-methoxyethyl)-4*H*-1,2,4-triazol-3-yl)thio)acetamide (1)**. ^1H NMR ($CDCl_3$+CD_3OD) δ 1.40 (t, *J* = 7.6Hz, 3H), 3.05 (q, *J* = 7.6Hz, 2H), 3.25 (s, 3H), 3.59 (t, *J* = 5.4Hz, 1H), 4.21 (s, 2H), 4.30 (t, *J* = 5.4Hz, 1H), 7.34 (s, 1H), 7.36 (dt, *J* = 8, 0.8Hz, 1H), 7.49 (dt, *J* = 8, 0.8Hz, 1H), 7.71 (d, *J* = 8.4Hz, 1H), 7.79 (d, *J* = 8Hz, 1H), 8.10 (s, 1H). Mass (ESI, +ve mode) calculated for $[C_{21}H_{23}N_6O_3S_2]^+$ = 471.13; found 471.16.

2,2',2''-((1,3,5-Triazin-2,4,6-triyl)tris(sulfanediyl))-*tris*-(*N*-(furan-2-ylmethyl)acetamide) (2). ^1H NMR ($CDCl_3$+CD_3OD) δ 3.98 (s, 6H), 4.42-4.40 (m, 6H), 6.22 (d, *J* = 3.2Hz), 6.30 (dd, *J* = 3.2, 0.8Hz, 3H), 7.33 (d, *J* = 0.8Hz, 3H), 7.98 (t, 1H). Mass (ESI, +ve) calculated for $[C_{24}H_{25}N_6O_6S_3]^+$ = 589.09; found 589.07.

Dibenzyl ((benzyloxy)carbonyl)glycylglutamate (3). ^1H NMR ($CDCl_3$) δ 2.10-1.90 (m, 1H), 2.20-2.29 (m, 1H), 2.33-2.48 (m, 2H), 3.80-3.92 (m, 2H), 4.67 (q, *J* = 5.2Hz, 1H), 5.08 (d, *J* = 2.4, 2H), 5.15 (s, 2H), 5.12 (s, 2H), 5.30 (bs, 1H), 6.71 (d, *J* = 7.6H, 1H), 7.29-7.40 (m, 15H). Mass (ESI, +ve mode) calculated for $[C_{29}H_{31}N_2O_7]^+$ = 519.2131; found 519.2327.

***N*,*N*'-(5-(Thiazol-2-ylcarbamoyl)-1,3-phenylene)bis(2-phenoxyacetamide) (4)**. ^1H NMR ($CDCl_3$+CD_3OD) δ 4.69 (s, 4H), 6.96-7.05 (m, 6H), 7.08 (d, *J* = 3.6Hz, 1H), 7.32 (t, *J* = 7.2 Hz, 4H), 7.49 (d, *J* = 3.6Hz, 1H), 8.03-8.07 (m, 2H), 8.32-8.35 (m, 1H). Mass (ESI, +ve mode) calculated for $[C_{26}H_{23}N_4O_5S]^+$ = 503.14; found 503.10.

(*E*)-2-(2-((5-(((4-Bromophenyl)sulfonamido)methyl)furan-2-yl)methylene)hydrazinyl)-*N*-(4-

methoxybenzyl)-2-oxoacetamide (5). ^{1}H NMR (DMSO-d_6+CD_3OD) δ 3.58 (s, 2H), 3.63 (s, 3H), 3.84 (s, 2H), 6.78 (d, *J* = 8.8Hz, 1H), 7.27-7.39 (m, 5H), 7.52 (d, *J* = 8.8Hz, 2H), 7.61 (s, 1H), 8.05 (d, *J* = 7.6Hz, 2H). Mass (ESI, +ve mode) calculated for $[C_{22}H_{22}BrN_4O_6S]^+$ = 549.0443 and 551.0423; found 549.06 and 551.17.

2-((6-Methyl-2-((2-oxo-2-phenylethyl)thio)pyrimidin-4-yl)thio)-*N*'-(2-phenylacetyl)acetohydrazide (6). ^{1}H NMR ($CDCl_3$) δ 2.27 (s, 3H), 3.58 (s, 2H), 3.71 (s, 2H), 3.85 (s, 2H), 6.78 (s, 1H), 7.25-7.36 (m, 5H), 7.50 (t, *J* = 7.2Hz, 2H), 7.61 (t, *J* = 7.2 Hz, 1H), 8.04 (d, *J* = 7.2 Hz, 2H). Mass (ESI, +ve mode) calculated for $[C_{23}H_{23}N_4O_3S_2]^+$ = 467.12; found 467.13.

(*E*)-3-(3-(4-Butoxy-2-methylphenyl)-1-phenyl-1*H*-pyrazol-4-yl)-2-cyano-*N*-(furan-2-ylmethyl) acrylamide (7). ^{1}H NMR ($CDCl_3$) δ 1.00 (t, *J*=7.2Hz, 3H), 1.57-1.48 (m, 1H), 1.83-1.76 (m, 1H), 2.27 (s, 3H), 4.01 (t, *J*=6.8Hz, 2H), 4.55 (d, *J*=5.6 Hz, 2H), 6.28 (d, *J*=3.2Hz, 1H), 6.33 (dd, *J*=2.8, 1.6Hz, 1H), 6.47 (t, *J*=5.6Hz, 1H), 6.81 (dd, *J*=8.4, 2.4 Hz, 1H), 6.86 (d, *J*=2Hz, 1H), 7.18 (d, *J*=8,4Hz, 1H), 7.38 (s, 1H), 7.39 (t, *J*=7.6Hz, 1H), 7.506 (t, *J*=7.6 Hz, 2H), 7.81 (d, *J*=7.6 Hz, 2H), 8.04 (s, 1H), 9.01 (s, 1H). Mass (ESI, +ve mode) calculated for $[C_{29}H_{29}N_4O_3]^+$ = 481.22; found 481.21.

(*Z*)-5-((3-(3-Fluoro-4-propoxyphenyl)-1-phenyl-1*H*-pyrazol-4-yl)methylene)-3-phenethyl-2-thioxothiazolidin-4-one (8). ^{1}H NMR ($CDCl_3$) δ 1.09 (t, *J* = 7.2Hz), 1.86-1.95 (m, 2H), 2.99-3.04 (m, 2H), 4.08 (t, *J* = 6.4Hz, 2H), 4.31-4.36 (m, 2H), 7.25-7.34 (m, 5H), 7.40 (t, *J* = 7.6Hz, 1H), 7.45 (dd, *J* = 11.6, 2Hz, 1H), 7.53 (t, *J* = 3.6Hz,2H), 7.72 (s, 1H), 7.79 (d, *J* = 3.6Hz, 2H), 8.16 (s, 1H). Mass (ESI, +ve mode) calculated for $[C_{30}H_{27}FN_3O_2S_2]^+$ = 544.15; found 544.13.

5-Chloro-*N*-(3-((4-chlorophenyl)amino)-3-oxopropyl)-2-((4-ethylbenzyl)thio)pyrimidine-4-carboxamide (9). ^{1}H NMR (CD_3OD) δ 1.21 (t, *J* = 7.6Hz, 3H), 2.59 (q, *J* = 7.6Hz, 2H), 2.70 (t, 6Hz, 2H), 3.36 (s, 2H), 3.74 (t, *J* = 6Hz, 2H), 7.07 (d, *J* = 8.4Hz, 2H), 7.26 (d, *J* = 8.4Hz, 2H), 7.36 (d, *J* = 8.4Hz, 2H), 7.41 (d, *J* = 8.4Hz, 2H), 7.48 (s, 1H), 8.64 (s, 1H). Mass (ESI, +ve mode) calculated for

$[C_{23}H_{23}Cl_2N_4O_2S]^+$ = 489.09; found 489.08.

2-((6-Isopropyl-4-oxo-3-phenethyl-3,5,6,8-tetrahydro-4*H*-pyrano[4',3':4,5]thieno[2,3-d]pyrimidin-2-yl)thio)-*N*-(3-methoxyphenyl)acetamide (10). ^{1}H NMR ($CDCl_3$) δ 1.04 *J* = 6.8Hz, 3H), 1.07 (d, *J* = 6.8Hz, 3H), 1.85-1.95 (m, 1H), 2.80-2.90 (m, 1H), 3.05 (t, *J* = 8Hz, 2H), 3.18 (dt, *J* = 14.8, 2.8Hz, 1H), 3.39-3.44 (m, 1H), 3.79 (s, 3H), 3.96 (s, 2H), 4.28 (dt, *J* = 9.2, 2.8Hz, 2H), 4.81 (dt, *J* = 15, 2.4Hz, 1H), 4.91 (d, *J* = 15Hz, 1H), 6.65 (dd, *J* = 8, 1.6Hz, 1H), 6.94 (dd, *J* = 8, 1.2Hz, 1H), 7.19 (t, *J* = 8Hz, 1H), 7.21-7.32 (m, 6H), 9.20 (s, 1H). Mass (ESI, +ve mode) calculated for $[C_{29}H_{32}N_3O_4S_2]^+$ = 550.18; found 550.15.

2-((6-Isopropyl-4-oxo-3-phenethyl-3,5,6,8-tetrahydro-4*H*-pyrano[4',3':4,5]thieno[2,3-d]pyrimidin-2-yl)thio)-*N*-(4-phenylbutan-2-yl)acetamide (11). ^{1}H NMR ($CDCl_3$) δ 1.03 (d, *J* = 6.8Hz, 3H), 1.06 (d, *J* = 6.8Hz, 3H), 1.15 (d, *J* = 6.4Hz, 3H), 1.65-1.78 (m, 2H), 1.85-1.95 (m, 1H), 2.55 (t, *J* = 8.4Hz, 2H), 2.78-2.87 (m, 1H), 3.04 (t, *J* = 7.6Hz, 2H), 3.16 (d, *J* = 17.6Hz, 1H), 3.35-3.42 (m, 1H), 3.75-3.87 (m, 2H), 3.98-4.05 (m, 1H), 4.22-4.35 (m, 2H), 4.75 (d, *J* = 14.4Hz, 1H), 4.84 (d, *J* = 14.4Hz, 1H), 6.63 (bt, *J* = 7.6Hz, 1H), 7.07-7.10 (m, 2H), 7.15 (t, *J* = 8Hz, 1H), 7.23 (t, *J* = 7.2Hz, 2H), 7.30-7.36 (m, 5H). Mass (ESI, +ve mode) calculated for $[C_{32}H_{38}N_3O_3S_2]^+$ = 576.24; found 576.26.

***N*-Benzyl-2-((6-isopropyl-4-oxo-3-phenethyl-3,5,6,8-tetrahydro-4*H*-pyrano[4',3':4,5]thieno[2,3-*d*]pyrimidin-2-yl)thio)acetamide (12) .** ^{1}H NMR ($CDCl_3$) δ 1.03 (d, *J* = 6.8Hz, 3H), 1.07 (d, *J* = 6.8Hz, 3H), 2.84-2.94 (m, 1H), 2.77-2.88 (m, 1H), 3.03 (t, *J* = 8Hz, 2H), 3.16 (dt, *J* = 16.4, 2.4Hz, 1H), 3.36-3.42 (m, 1H), 3.91 (s, 2H), 4.27 (dt, *J* = 8, 4.8Hz, 2H), 4.44 (d, *J* = 5.6Hz, 2H), 4.77 (dt, *J* = 14.8, 2.4Hz, 1H), 4.86 (d, *J* = 14.8Hz, 2H), 6.93 (bt, 1H), 7.19-7.24 (m, 2H), 7.24 (d, *J* = 5.2Hz, 4H), 7.29 (d, *J* = 4.4Hz, 4H). Mass (ESI, +ve mode) calculated for $[C_{29}H_{32}N_3O_3S_2]^+$ = 534.19; found 534.21.

***S*-Benzyl-*N*-(2-((2-oxo-4-propyl-2*H*-chromen-7-yl)oxy)acetyl)cysteine (13)**. ^{1}H NMR ($CDCl_3$) δ

1.05 (t, *J* = 7.6Hz), 1.66-1.77 (m, 2H), 2.70 (t, *J* = 7.6Hz, 2H), 2.93-3.03 (m, 2H), 4.61 (s, 2H), 3.73 (s, 2H), 4.86 (q, *J* = 7.6Hz, 1H), 6.17 (s, 1H), 6.90 (d, *J* = 2.4Hz, 1H), 6.93 (dd, *J* = 8, 1.6Hz, 1H), 7.19-7.33 (m, 6H), 7.56 (d, *J* = 9.2Hz, 1H). Mass (ESI, +ve mode) calculated for $[C_{24}H_{26}NO_6S]^+$ = 456.15; found 456.12.

2-(2-(4-Methoxyphenyl)-2-oxoethylthio)-6-methylpyrimidin-4(3*H*)-one (15A). A mixture of compound **14** (300 mg, 2,1 mmol), 2-bromo-1-(4-methoxyphenyl)ethanone (483 mg, 2.1 mmol) and potassium carbonate (291 mg, 2.1 mmol) was stirred in anhydrous *N*,*N*-dimethylformamide (3 mL) at room temperature for 12 h. Completion of the reaction was monitored by TLC. The reaction content was poured on cold water (5 mL) and extracted with ethyl acetate (3 x 10 mL). The organic layers were combined together, washed with brine (1 x 10 mL), dried over anhydrous sodium sulfate and the solvent was evaporated to dryness. The crude mixture was purified by column chromatography (hexanes:ethyl acetate gradient) to obtain pure compound **15A** as a pale yellow (306 mg, 50%). ^{1}H NMR (DMSO-d_6) δ 12.659 (s, 1H), 8.0235 (d, *J* = 9.2 Hz, 2H), 7.0745 (d, *J* = 9.2 Hz, 2H), 5.931 (s, 1H), 4.699 (s, 2H), 3.855 (s, 3H), 1.981 (s br., 3H).

2-(2-(4-(Diethylamino)phenyl)-2-oxoethylthio)-6-methylpyrimidin-4(3*H*)-one (15B). Compound **15B** was synthesized using the method described for compound **15A** starting from compound **14** (200 mg, 1.4 mmol) and 2-bromo-1-(4-(diethylamino)phenyl)ethanone (380 mg, 1.4 mmol). The product was obtained as an orange solid (256 mg, 55%). ^{1}H NMR (DMSO-d_6) δ 7.843 (d, *J* = 8.8 Hz, 2H), 6.714 (d, *J* = 9.2 Hz, 2H), 5.918 (s, 1H), 4.638 (s, 2H), 3.433 (q, *J* = 7.2 Hz, 4H), 2.046 (s br., 3H), 1.122 (t, *J* = 7.0 Hz, 6H).

6-Methyl-2-(2-morpholino-2-oxoethylthio)pyrimidin-4(3*H*)-one (15C). Compound **15C** was synthesized using the method described for compound **15A** starting from compound **14** (300 mg, 2.1 mmol) and 2-bromo-1-morpholinoethanone (345 mg, 2.1 mmol) heating at 70 °C for 5 h. The product was obtained as a yellow solid (307 mg, 54%). ^{1}H NMR (DMSO-d_6) δ 5.987 (s, 1H), 4.153 (s, 2H),

3.64-3.60 (m, 2H), 3.58-3.54 (m, 4H), 3.48-3.43 (m, 2H), 2.152 (s, 3H).

6-Methyl-2-(2-morpholinoethylthio)pyrimidin-4(3*H*)-one (15D). Compound **15D** was synthesized using the method described for compound **15A** starting from compound **14** (250 mg, 1.7 mmol) and 4-(2-bromoethyl)morpholine (327 mg, 1.7 mmol) heating at 70 °C for 5.5 h. The product was obtained as a pale yellow solid (256 mg, 57%). ^{1}H NMR (DMSO-d_6) δ 5.943 (s, 1H), 3.571 (t, J = 4.6 Hz, 4H), 3.250 (t, J = 7.0 Hz, 4H), 2.46-2.40 (m, 4H), 2.145 (s, 3H).

4-(2-(4-Methyl-6-oxo-1,6-dihydropyrimidin-2-ylthio)acetyl)benzonitrile (15E). Compound **15E** was synthesized using the method described for compound **15A** starting from compound **14** (300 mg, 2.1 mmol) and 4-(2-bromoacetyl)benzonitrile (472 mg, 2.1 mmol). The product was obtained as a pale yellow solid (325 mg, 54%). ^{1}H NMR (DMSO-d_6) δ 7.844 (d, J = 8.4 Hz, 2H), 7.614 (d, J = 8.4 Hz, 2H), 5.917 (s, 1H), 4.721 (s, 2H), 1.897 (s br., 3H).

2-(4-Chloro-6-methylpyrimidin-2-ylthio)-1-(4-methoxyphenyl)ethanone (16A). $POCl_3$ (1.0 mL, 1.645g, 10.7mmol) was added to compound **15A** (100 mg, 0.38 mmol) and the mixture was heated at 70°C with stirring. After 15 min, the reaction was quenched with sodium bicarbonate saturated solution (10 mL) and extracted with ethyl acetate (10 mL). The organic phase was washed with water (3 x 10 mL) and dried over anhydrous sodium sulfate. The solvent was evaporated to obtain a crude mixture which was purified by column chromatography (chloroform/methanol gradient) to yield compound **16A** as an yellow solid (85 mg, 80%). ^{1}H NMR (DMSO-d_6) δ 8.054 (d, J = 9.2 Hz, 2H), 6.973 (d, J = 8.8 Hz, 2H), 6.871 (s, 1H), 4.604 (s, 2H), 3.893 (s, 3H), 2.391 (s, 3H).

2-(4-Chloro-6-methylpyrimidin-2-ylthio)-1-(4-(diethylamino)phenyl)ethanone (16B). Compound **16B** was synthesized using the method described for compound **16A** heating at 70°C for 20 min obtained as a solid (90 mg, 85%). ^{1}H NMR (DMSO-d_6) δ 7.954 (d, J = 8.8 Hz, 2H), 6.843 (s, 1H), 6.644 (d, J = 9.2 Hz, 2H), 4.590 (s, 2H), 3.438 (q, J = 7.0 Hz, 4H), 2.388 (s, 3H), 1.216 (t, J = 7.0 Hz, 6H).

2-(4-Chloro-6-methylpyrimidin-2-ylthio)-1-morpholinoethanone (16C). Compound **16C** was synthesized using the method described for compound **16A** heating at 70 °C for 10 min obtained as a solid (83 mg, 78%). ^{1}H NMR (DMSO-d_6) δ 6.889 (s, 1H), 4.064 (s, 2H), 3.758-3.646 (m, 8H), 2.441 (s, 3H).

4-(2-(4-Chloro-6-methylpyrimidin-2-ylthio)ethyl)morpholine (16D). Compound **16D** was synthesized using the method described for compound **16A** heating at 75°C for 20 min obtained as a white solid (75 mg, 70%). ^{1}H NMR ($CDCl_3$) δ 6.862 (s, 1H), 3.76-3.70 (m, 4H), 3.32-3.26 (m, 2H),2.74-2.68 (m, 2H), 2.59-2.53 (m, 4H), 2.433 (s, 3H).

4-(2-(4-Chloro-6-methylpyrimidin-2-ylthio)acetyl)benzonitrile (16E). Compound **16E** was synthesized using the method described for compound **16A** and the product was obtained as a pale yellow solid (74 mg, 75%). ^{1}H NMR (DMSO) δ 8.156 (d, J = 8.8 Hz, 2H), 7.813 (d, J = 8.8 Hz, 2H), 6.874 (s, 1H), 4.549 (s, 2H), 2.351 (s, 3H).

2-Phenylacetohydrazide (18). To a solution of methyl 2-phenylacetate **17** (500 mg, 3.3 mmol) in anhydrous methanol (25 mL), hydrazine hydrate (533 mg, 16.6 mmol) was added in portions over ten minutes period under nitrogen atmosphere at room temperature, and the reaction mixture was stirred for further 16 h. After completion of the reaction (monitored by TLC), the solvent was evaporated under reduced pressure. The crude residue was treated with diethyl ether (10 mL) to afford compound **18** as white precipitate that was collected by filtration and dried under vacuum (400 mg, 80 %). ^{1}H NMR ($CDCl_3$) δ 3.57 (s, 2H), 3.84 (s, 2H), 6.66 (bs, 1H), 7.25 – 7.38 (m, 5H).

2-Chloro-*N*'-(2-phenylacetyl)acetohydrazide (19). 2-Chloroacetyl chloride (0.23 mL, 2.9 mmol) was added to a solution of compound **18** (400 mg, 2.6 mmol) and *N*,*N*-di-isopropyl ethylamine (0.46 mL, 2.6 mmol) in anhydrous dichloromethane (20 mL) at –10 °C slowly under inert atmosphere. The reaction mixture was stirred at 0 °C and after 30 min, it was quenched with saturated sodium bicarbonate solution (10 mL), the organic phase was collected and washed with water (3 x 10 mL) and

dried over anhydrous sodium sulfate. After evaporation of the solvent, the crude mixture was purified by column chromatography (chloroform/methanol gradient) to yield compound **19** as a white solid (400 mg, 66%). ^{1}H NMR (DMSO-d_6) δ 3.48 (s, 2H), 4.12 (s, 2H), 7.212 – 7.26 (m, 1H), 7.28-7.33 (m, 4H), 10.28 (bs, 1H), 10.30 (bs, 1H).

***S*-2-(2-(2-Phenylacetyl)hydrazinyl)ethyl ethanethioate (20)**. To a solution of compound **19** (400 mg, 1.76 mmol) in ethanol (12 mL), potassium thioacetate (705 mg, 6.17 mmol) was added and the mixture was stirred at room temperature for 16 h. After completion of the reaction (TLC monitored), the mixture was diluted with ethyl acetate and THF, washed with water and brine, and dried over anhydrous sodium sulfate. The solvent was evaporated under reduced pressure and the crude was purified by column chromatography (chloroform methanol gradient) to yield compound **20** as a brown solid (320 mg, 68%). ^{1}H NMR (DMSO-d_6) δ 2.36 (s, 3H), 3.45 (s, 2H), 3.65 (s, 2H), 7.21 - 7.25 (m, 1H), 7.27-7.31 (m, 4H), 10.15 (bs, 1H), 10.18 (bs, 1H).

2-Mercapto-*N*'-(2-phenylacetyl)acetohydrazide (21). To a solution of compound **20** (200 mg, 0.75 mmol) in methanol (5 mL), K_2CO_3 (207 mg, 1.5 mmol) was added and the mixture was stirred at room temperature for 1 h. The reaction mixture was diluted with ethyl acetate (10 mL) and THF (10 mL), washed with water and brine, and dried over anhydrous sodium sulphate. The solvent was evaporated and the crude mixture was purified by column chromatography (chloroform - methanol gradient) to obtain compound **21** as a white solid (120 mg, 71.4 %). ^{1}H NMR (DMSO-d_6) δ 2.79 (t, J = 8 Hz, 1H), 3.15 (d, J = 8 Hz, 2H), 3.47 (bs, 2H), 7.20-7.26 (m, 1H), 7.28-7.36 (m, 4H), 10.06 (d, J = 2 Hz, 1H), 10.20 (d, J = 2 Hz,, 1H).

2-(2-(2-(4-Methoxyphenyl)-2-oxoethylthio)-6-methylpyrimidin-4-ylthio)-*N*'-(2-phenylacetyl)acetohydrazide (22). To a solution of compound **21** (68 mg, 0.22 mmol) and **16A** (50 mg, 0.22 mmol) in anhyd acetonitrile (10 mL), triethylamine (0.034 mL, 0.24 mmol) was added and the reaction mixture was stirred at 75 °C for 6 h. Reaction mixture was quenched with cold water (5

mL), and extracted with ethyl acetate (3 ×10 mL). Combined organic layers were washed with brine (10 mL), dried with anhydrous sodium sulfate and evaporated. The residue was purified by column chromatography (hexanes/ethyl acetate gradient) to obtain **22** as a pale white solid (44 mg, 40%). ^{1}H NMR (DMSO-d_6) δ 10.25 (s,1H), 10.20 (s, 1H), 8.038 (d, J = 8.8 Hz, 2H), 7.307-7.238 (m, 5H), 7.062-7.040 (m, 3H), 4.742 (s, 2H), 3.861 (s, 2H), 3.840 (s, 3H), 3.454 (s, 2H), 2.228 (s, 3H). ^{13}C NMR (DMSO-d_6) δ 192.43, 169.11, 168.75, 168.51, 165.92, 165.41, 163.33, 135.60, 130.72, 128.96, 128.78, 128.18, 126.47, 113.93, 113.01, 55.53, 37.80 30.62, 23.06. Mass (ESI, +ve) calculated for $[C_{24}H_{25}N_4O_4S_2]^+$ = 497.13, found 497.23.

2-(2-(2-(4-(Diethylamino)phenyl)-2-oxoethylthio)-6-methylpyrimidin-4-yl-thio)-*N*'-(2-^phenylacetyl)acetohydrazide (23). Compound **23** was synthesized using the method described for compound **22**. Briefly to a solution of compounds **21** (78 mg, 0.22 mmol) and **16B** (50 mg, 0.22 mmol) in anhyd acetonitrile (10 mL), triethylamine (0.032 mL, 0.23 mmol) was added and stirred at 90 °C for 4 h. Compound **23** was obtained as a white solid (50 mg, 41%) ^{1}H NMR (DMSO-d_6) δ 10.22 (s, 1H), 10.19 (s,1H), 7.86 (d, J = 8.4 Hz, 2H), 7.27-7.22 (m, 5H), 7.06 (s, 1H), 6.69 (d, J = 8.0 Hz, 2H), 4.65 (s, 2H), 3.91 (s, 2H), 3.45-3.40 (m, 6H), 2.26 (s, 3H), 1.12 (t, J = 6.4 Hz, 6H). ^{13}C NMR (DMSO-d_6) δ 190.87, 169.41, 168.70, 168.41, 165.94, 165.36, 151.11, 135.60, 130.85, 130.85, 128.95, 128.95, 128.16, 128.16, 126.44, 122.43, 112.97, 110.14, 43.83, 37.41, 30.68, 23.11, 12.34. Mass (ESI, +ve) calculated for $[C_{27}H_{31}N_5O_3S_2]^+$ = 538.19, found 538.25.

2-(6-Methyl-2-(2-morpholino-2-oxoethylthio)pyrimidin-4-ylthio)-*N*'-(2-phenylacetyl) acetohydrazide (24). Compound **24** was synthesized using the method described for compound **22**; Briefly, to a solution of compound **21** (64 mg, 0.22 mmol) and **16C** (50 mg, 0.22 mmol) in anhyd acetonitrile (10 mL), triethylamine (0.032 mL, 0.24 mmol) was added and stirred at 70 °C for 30 min. Compound **24** was obtained as a yellow solid (42 mg, 40%). ^{1}H NMR (DMSO-d_6) δ 10.19 (s, 1H), 10.17 (s, 1H), 7.30-7.20 (m, 5H), 7.08 (s, 1H), 4.18 (s, 2H), 3.96 (s, 2H), 3.58-3.51 (m, 6H), 3.48-3.42

(m, 4H), 2.29 (s, 3H). ^{13}C NMR (DMSO-d_6) δ 169.32, 168.75, 168.21, 166.04, 166.01, 165.26, 128.88, 128.20, 128.08, 126.40, 112.97, 65.96, 65.90, 45.81, 41.89, 33.34, 30.57, 23.04; Mass (ESI, +ve) calculated for $[C_{21}H_{26}N_5O_4S_2]^+$ = 476.14, found 476.21.

2-(6-Methyl-2-(2-morpholinoethylthio)pyrimidin-4-yl-thio)-*N*'-(2-phenylacetyl)acetohydrazide (25). Compound **25** was synthesized using the method described for compound **22**; briefly, compounds **21** (61 mg, 0.22 mmol) and **16D** (50 mg, 0.22 mmol) were dissolved in anhyd acetonitrile (10 mL) and triethylamine (0.034 mL, 0.024 mmol) was added. The reaction mixture was stirred at 90 °C for 4.5 h. Compound **25** was obtained as a white solid (31 mg, 30%). ^{1}H NMR (DMSO-d_6) δ 10.34 (s, 1H), 10.250 (s, 1H), 7.315-7.203 (m, 5H), 7.062 (s, 1H), 3.957 (s, 2H), 3.533 (t, J = 4.4 Hz, 4H), 3.469 (s, 2H), 3.236 (t, J = 7.2 Hz, 2H), 2.596 (t, J = 7.2 Hz, 2H), 2.449-2.372 (m, 4H), 2.291 (s, 3H). ^{13}C NMR (DMSO-d_6) δ 169.94, 168.67, 168.31, 165.91, 165.34, 135.54, 128.87, 128.11, 126.40, 112.73, 65.96, 57.16, 52.93, 40.07, 30.63, 27.04, 23.08; Mass (ESI, +ve) calculated for $[C_{21}H_{28}N_5O_3S_2]^+$ = 462.16, found 462.24.

2-(2-(2-(4-Cyanophenyl)-2-oxoethylthio)-6-methylpyrimidin-4-yl-thio)-*N*'-(2-phenylacetyl) acetohydrazide (26). Compound **26** was synthesized using the method described for compound **22**; to a solution of compound **21** (55 mg, 0.22 mmol) and **16E** (50 mg, 0.22 mmol) in anhyd acetonitrile (10 mL), triethylamine (0.034 mL, 0.24 mmol) was added and stirred at 90 °C for 1.5 h. Compound **26** was obtained as a white solid compound (43 mg, 40%) . ^{1}H NMR (DMSO-d_6) δ 10.193 (s, 1H), 10.153 (s, 1H), 8.182 (d, J = 8.4 Hz, 2H), 8.002 (d, J = 8.0 Hz, 2H), 7.290-7.199 (m, 5H), 7.066 (s, 1H), 4.805 (s, 2H), 3.841 (s, 2H), 3.448 (s, 2H), 2.186 (s, 3H). ^{13}C NMR (DMSO-d_6) δ 203.26, 178.13, 175.25, 174.88, 148.81, 144.98, 142.09, 138.34, 138.27, 137.55, 135.84, 127.49, 124.67, 122.50, 40.06, 32.35; Mass (ESI, +ve) calculated for $[C_{24}H_{22}N_5O_3S_2]$ = 492.12, found 492.22.

Ethyl 3-benzyl-4-oxo-2-thioxo-1,2,3,4-tetrahydropyrimidine-5-carboxylate (28). A mixture of benzyl thiourea **27** (2.0 gm, 12.0 mmol), diethyl (ethoxymethylene)malonate (2.6 gm, 12.0 mmol),

potassium carbonate (3.2 gm, 24.0 mmol) and pyridine (0.1 mL) in anhyd DMF (20 mL) was stirred at 120° C in a microwave reactor (100W) for 1.0 hr. The reaction mixture was cooled to rt, and the solvent was evaporated. The crude reaction mixture was dissolved in ethyl acetate, washed with 1 N HCl solution, dried (anhyd Na_2SO_4) and concentrated under reduced pressure. The crude product was purified by column chromatography (ethyl acetate: hexane 70:30) to give compound **28** (1.91 g, 55%) as a yellow solid. ^{1}H NMR (DMSO-d_6) δ 13.18 (s, 1H), 8.03 (s, 1H), 7.33-7.21(m, 5H), 4.18 (q, J =7.06, 2H), 1.24 (t, J = 7.06 Hz, 3H).

3-Benzyl-4-oxo-*N*-(3-phenylpropyl)-2-thioxo-1,2,3,4-tetrahydropyrimidine-5-carboxamide (29). A stirred solution of trimethyl aluminum (6.85 mL, 13.7 mmol, 2 M solution in toluene) in anhyd dichloromethane (5 mL) was treated with compound **28** (1 gm, 3.4 mmol) in anhyd dichloromethane (20 mL) at 0° C. After stirring for 30 min, 3-phenyl-propylamine (1.92 mL, 13.7 mmol) in anhyd dichloromethane (5 mL) was added and the mixture was stirred overnight at rt. The reaction mixture was then quenched with 1N NaOH solution at 0 °C, and the organic layer was washed with water (15 mL), brine (15 mL) and dried over anhyd Na_2SO_4. Combined organic layers were concentrated and the crude product was purified by column chromatography (ethyl acetate:hexanes, 60:40) to give compound **29** (0.72 g, 55 %) as a white solid. ^{1}H NMR (DMSO-d_6) δ 13.31 (s, 1H), 8.70 (t, J = 5.8Hz, 1H), 8.06 (s, 1H), 7.38 – 7.04 (m, 10H), 5.57 (s, 2H), 3.26 (dd, J = 13.2, 6.8 Hz 2H), 2.58 (t, J = 7.6 Hz, 2H), 1.85 – 1.70 (m, 2H).

1-Benzyl-6-oxo-2-(2-oxo-2-phenylethylthio)-*N*-(3-phenylpropyl)-1,6-dihydropyrimidine-5-carboxamide (30). To a solution of **29** (30 mg, 0.079 mmol) and 2-bromo-1-phenylethanone (15 mg, 0.079 mmol) in anhyd AcCN (10 mL), triethylamine (0.010 mL, 0.079 mmol) was added, and the mixture was stirred at 60 °C for 45 min. The reaction mixture was quenched with cold water (5 mL), and extracted with ethyl acetate (3×0 mL). Combined organic layers were washed with brine (10 mL), dried (anhyd Na_2SO_4), and concentrated to furnish crude product which was then purified by column

chromatography (EtOAc:Hexanes, 1:1) as a mobile phase to obtain compound **30** as a white solid (16 mg, 41%). ^{1}H NMR (DMSO-d_6) δ 8.90 (t, J = 5.6 Hz, 1H), 8.39 (s, 1H), 8.04 (d, J = 8.0 Hz, 2H), 7.69 (t, J = 8.0 Hz, 1H), 7.57 (t, J = 7.5 Hz, 2H), 7.42 – 7.13 (m, 9H), 5.41 (s, 2H), 4.98 (s, 2H), 3.32-3.24 (m, 2H), 2.59 (t, J =6.0 Hz, 2H), 1.86 – 1.71 (m, 2H). ^{13}C NMR (DMSO) δ 192.33, 165.94, 161.01, 155.01, 141.41, 135.68, 134.23, 128.84, 128.69, 128.29, 128.26, 128.22, 112.41, 47.91, 40.15, 39.94, 38.23, 32.50, 30.68; Mass (ESI, +ve) calculated for $[C_{29}H_{28}N_3O_3S]^+$ = 498.19, found 498.17.

1-Benzyl-2-(2-(4-methoxyphenyl)-2-oxoethylthio)-6-oxo-*N*-(3-phenylpropyl)-1,6 dihydropyrimidine-5-carboxamide (31). Compound **31** was synthesized using the method described for compound **30**; to a solution of compound **29** (30 mg, 0.079 mmol) and 4-(2-bromoacetyl)benzonitrile (18 mg, 0.079 mmol) in anhyd acetonitrile (10 mL), triethylamine (0.012 mL, 0.0805 mmol) was added and the reaction mixture was stirred at 70 °C for 30 min. Compound **31** as a brown solid (17 mg, 41%). ^{1}H NMR (DMSO-d_6) δ 8.90 (t, J = 8.0 Hz ,1H), 8.41 (s, 1H), 8.02 (d, J = 8.0 Hz, 2H), 7.41 – 7.27 (m, 6H), 7.25 (d, J = 7.2 Hz, 2H), 7.09 (d, J = 8.8 Hz, 2H), 5.40 (s, 2H), 4.93 (s, 2H), 3.86 (s, 2H), 3.32-3.27 (dd, J = 13.2, 6.4 Hz 2H), 2.60 (t, J = 7.4 Hz 2H), 1.83 – 1.75 (m, 2H). ^{13}C NMR (DMSO-d_6) δ 190.52, 166.09, 163.55, 161.99, 161.02, 155.05, 141.41, 134.25, 130.73, 128.67, 128.45, 128.26, 128.21, 127.71, 126.90, 125.72, 114.06, 112.35, 55.61, 47.84, 38.22, 33.84, 32.50, 31.64, 30.67; Mass (ESI, +ve) calculated for $[C_{30}H_{30}N_3O_4S]^+$ = 528.20, found 528.24.

1-Benzyl-6-oxo-2-(2-oxo-2-(2-(2-phenylacetyl)hydrazinyl)ethylthio)-*N*-(3-phenylpropyl)-1,6-dihydropyrimidine-5-carboxamide (32). Compound **32** was synthesized using the method described for compound **30**; to a solution of compound **29** (30 mg, 0.08 mmol) and 2-chloro-*N*'-(2-phenylacetyl)acetohydrazide (17 mg, 0.08 mmol) in anhyd acetonitrile (10 mL), triethylamine (0.012 mL, 0.087 mmol) was added and the reaction mixture was stirred at 85 °C for 20 min. After work-up and purification, compound **32** was obtained as a white solid compound (13 mg, 30%). ^{1}H NMR (DMSO-d_6) δ 10.21 (s, 1H), 8.96 (t , J = 6.0 Hz, 1H), 8.56 (s, 1H), 7.40 – 7.16 (m, 15H), 5.34 (s, 2H),

4.06 (s, 2H), 3.46 (s, 2H), 3.30 (dd, *J* = 13.0, 6.6 Hz, 2H), 2.61 (t, *J* = 7.6 Hz, 3H), 1.85 – 1.77 (m, 2H). ^{13}C NMR (DMSO-d_6) δ 169.04, 166.01, 165.29, 162.31, 161.25, 155.43, 141.54, 135.67, 134.27, 129.13, 128.85, 128.44, 128.37, 127.01, 126.66, 125.91, 112.49, 47.89, 34.38, 32.64, 30.81; Mass (ESI, +ve) calculated for $[C_{31}H_{32}N_5O_4S]^+$ = 570.22, found 570.26.

1-Benzyl-2-(2-morpholinoethylthio)-6-oxo-*N*-(3-phenylpropyl)-1,6-dihydropyrimidine-5-carboxamide (33). Compound **33** was synthesized using the method described for compound **30**; to a solution of compound **29** (40 mg, 0.10 mmol) and 4-(2-chloroethyl)morpholine (19 mg, 0.10 mmol) in anhyd acetonitrile (10 mL), triethylamine (38 μL, 0.26 mmol) was added and the reaction mixture was stirred at 80 °C for 60 min. After the work-up of the reaction mixture and purification, compound **33** was obtained as a yellow solid (20 mg, 38%). ^{1}H NMR (CD_3OD) δ 8.67 (s, 1H), 7.36 – 7.11 (m, 10H), 5.40 (s, 2H), 3.68 – 3.62 (m, 4H), 3.48-3.37 (m, 4H), 2.72 – 2.65 (m, 4H), 2.53 – 2.46 (m, 4H), 1.95-1.86 (m, 2H). ^{13}C NMR (CD_3OD) δ 169.15, 165.49, 163.27, 157.14, 142.76, 135.74, 129.79, 129.48, 129.47, 129.01, 128.48, 128.47, 126.97, 113.19, 67.81, 58.02, 54.51, 39.89, 34.23, 32.21, 30.64; Mass (ESI, +ve) calculated for $[C_{27}H_{33}N_4O_3S]^+$ = 493.23, found 493.27.

Ethyl-2-(1-benzyl-6-oxo-5-(3-phenylpropylcarbamoyl)-1,6-dihydropyrimidin-2-ylthio)acetate (34). Compound **34** was synthesized using the method described for compound **30**; to a solution of compound **29** (100 mg, 0.26 mmol) and ethyl 2-bromoacetate (0.032 mL, 0.29 mmol) in anhyd acetonitrile (10 mL), triethylamine (0.042 mL, 0.29 mmol) was added and the reaction mixture was stirred at 70 °C for 20 min. Following work-up and purification of the crude, compound **34** was obtained as a white solid (50 mg, 41%). ^{1}H NMR (CD_3OD) δ 8.61 (s, 1H), 7.35 – 7.11 (m, 10H), 5.41 (s, 2H), 4.18 (q, *J* = 7.2 Hz, 2H), 4.08 (s, 2H), 3.39 (t, *J* = 7.0 Hz, 2H), 2.70-2.64 (m, 2H), 1.90 (m, 2H), 1.24 (t, *J* = 7.2Hz, 3H). ^{13}C NMR (CD_3OD) δ 165.23, 163.02, 156.85, 142.77, 135.44, 129.81, 129.44, 129.43, 129.09, 128.47, 126.93, 113.59, 63.05, 39.89, 34.19, 32.12, 14.44; Mass (ESI, +ve) calculated for $[C_{25}H_{27}N_3O_4S]^+$ = 466.1801, found 466.1801.

1-Benzyl-2-(2-(4-(diethylamino)phenyl)-2-oxoethylthio)-6-oxo-*N*-(3-phenylpropyl)-1,6-dihydropyrimidine-5-carboxamide (35). Compound **35** was synthesized using the method described for compound **30**; to a solution of compound **29** (50 mg, 0.13 mmol) and 2-bromo-1-(4-(diethylamino)phenyl)ethanone (35 mg, 0.13 mmol) in anhyd acetonitrile (10 mL), triethylamine (0.02 mL, 0.13 mmol) was added and stirred at 70 °C for 30 min. Following work-up and purification of the crude, compound **35** was obtained as a white solid (15 mg, 20%). ^{1}H NMR (DMSO-d_6) δ 8.93 (t, J = 5.6 Hz, 1H), 8.46 (s, 1H), 7.84 (d, J = 8.8 Hz, 2H), 7.42 – 7.16 (m, 10H), 6.72 (d, J = 9.2 Hz, 2H), 5.40 (s, 2H), 4.85 (s, 2H), 3.46-3.40 (m, 4H), 3.28 (dd, J = 13.0, 6.6 Hz, 2H), 2.62-256 (m, 2H), 1.85-1.74 (m, 2H), 1.12 (t, J = 7.0 Hz, 6H). ^{13}C NMR (DMSO-d_6) δ 189.43, 167.13, 162.85, 161.75, 151.99, 142.08, 134.92, 131.52, 129.37, 128.96, 128.90, 127.54, 126.43, 122.66, 112.85, 110.90, 44.57, 33.16, 31.34, 12.98; Mass (ESI, +ve) calculated for $[C_{33}H_{37}N_4O_3S]^+$ = 569.26, found 569.29.

1-Benzyl-2-(2-(4-hydroxyphenyl)-2-oxoethylthio)-6-oxo-*N*-(3-phenylpropyl)-1,6-dihydropyrimidine-5-carboxamide (36). Compound **36** was synthesized using the method described for compound **30**; to a solution of compound **29** (40 mg, 0.10 mmol) and 2-bromo-1-(4-hydroxyphenyl)ethanone (24 mg, 0.10 mmol) in anhyd acetonitrile (10 mL), triethylamine (0.015 mL, 0.11 mmol) was added and the reaction mixture was stirred at 60 °C for 70 min. Reaction mixture was worked-up and purified to obtain **36** as a white solid (25 mg, 46%) ^{1}H NMR ($CDCl_3$) δ 9.30 (t, J = 5.8 Hz, 1H), 8.81 (br s, 1H), 8.67 (s, 1H), 7.97 (d, J = 8.8 Hz, 2H), 7.46-7.00 (m, 12H), 5.44 (s, 2H), 4.78 (s, 2H), 3.46 (dd, J = 13.2, 6.4 Hz, 2H), 2.71 (t, J = 7.8 Hz, 2H), 2.00-1.91 (m, 2H). ^{13}C NMR ($CDCl_3$) δ 189.10, 165.38, 162.85, 161.54, 160.83, 155.22, 140.32, 132.51, 130.16, 127.89, 127.41, 127.39, 127.34, 126.70, 124.94, 114.87, 111.21, 47.41, 40.12, 38.19, 32.21, 29.92; Mass (ESI, +ve) calculated for $[C_{29}H_{28}N_3O_4S]^+$ = 514.18, found 514.18.

1-Benzyl-2-(2-(4-cyanophenyl)-2-oxoethylthio)-6-oxo-*N*-(3-phenylpropyl)-1,6-dihydropyrimidine-5-carboxamide (37). Compound **37** was synthesized using the method described

for compound **30**; to a solution of compound **29** (35 mg, 0.092 mmol) and 4-(2-bromoacetyl)benzonitrile (20 mg, 0.092 mmol) in anhyd acetonitrile (10 mL), triethylamine (0.01 mL, 0.10 mmol) was added and the reaction mixture was stirred at 70 °C for 30 min. Reaction mixture was worked-up and the crude was purified to obtain compound **37** as a white solid (24 mg, 50%). ^{1}H NMR (DMSO-d_6) δ 8.87 (t , J = 5.8 Hz, 1H), 8.35 (s, 1H), 8.16 (d, J = 8.4 Hz, 2H), 8.05 (d, J = 8.0 Hz, 2H), 7.40 – 7.13 (m, 9H), 5.38 (s, 2H), 4.95 (s, 2H), 3.32-3.24 (dd, J = 13.2, 7.0 Hz, 2H), 2.58 (t, J = 7.8 Hz, 2H), 1.83-1.75 (m, 2H); ^{13}C NMR (DMSO-d_6) δ 192.24, 165.58, 161.85, 161.85, 160.88, 155.05, 141.33, 139.03, 134.09, 132.77, 128.79, 128.61, 128.18, 128.14, 127.67, 126.83, 126.59, 125.65, 117.98, 115.39, 112.42, 47.85, 38.16, 32.41, 30.58; Mass (ESI, +ve) calculated for $[C_{30}H_{27}N_4O_3S]^+$ = 523.18, found 523.20.

1-Benzyl-2-(2-morpholino-2-oxoethylthio)-6-oxo-*N*-(3-phenylpropyl)-1,6-dihydropyrimidine-5-carboxamide compound (38). Compound **38** was synthesized using the method described for compound **30**; to a solution of compound **29** (40 mg, 0.010 mmol) and 4-(2-bromoacetyl)morpholine (17 mg, 0.010 mmol) in anhyd acetonitrile (10 mL), triethylamine (18 μL, 0.21 mmol) was added and the reaction mixture was stirred at 75 °C for 30 min. Reaction was worked-up and the crude was purified to obtain **38** as a white solid (21 mg, 40%). ^{1}H NMR (DMSO-d_6) δ 8.93 (t, J = 5.8 Hz, 1H), 8.56 (s, 1H), 7.43-7.10 (m, 9H), 5.36 (s, 2H), 4.35 (s, 2H), 3.65-3.58 (m, 2H), 3.57-3.50 (m, 4H), 3.46-3.40 (m, 2H), 3.29 (dd, J = 13.4, 7.4 Hz, 2H), 2.61 (t, J = 7.6 Hz 2H), 1.85-1.75 (m, 2H). ^{13}C NMR (DMSO-d_6) δ 166.24, 164.70, 162.03, 160.92, 141.28, 134.14, 128.58, 128.19, 128.14, 127.59, 126.78, 125.66, 112.34, 65.85, 47.69, 45.81, 42.05, 38.20, 35.86, 32.43, 30.54, 18.11; Mass (ESI, +ve) calculated for $[C_{27}H_{31}N_4O_4S]^+$ = 507.21, found 507.25.

Ethyl-2-(2-oxo-2-(2-(2-phenylacetyl)hydrazinyl)ethylthio)-pyrimidin-4-one-5-carboxylate (40). A mixture of compound **39** (100 mg, 0.50 mmol), 2-chloro-*N*'-(2-phenylacetyl)acetohydrazide (112 mg, 0.50 mmol) and potassium carbonate (69 mg, 0.5 mmol) in anhyd acetone (3 mL) was stirred at rt for

16 h. Then the solvent was evaporated, the crude was poured onto cold water (5 mL), the resulting precipitate was washed with water (10 mL), and diethyl ether (10 mL) to yield compound **40** as a white solid (117 mg, 60%). ^{1}H NMR (DMSO-d_6) δ 10.23 (s, 2H), 8.39 (s, 1H), 7.27 (m, 5H), 4.19 (q, J =7.06, 2H), 3.97 (s, 2H), 3.47 (s, 2H), 1.25 (t, J=7.06 Hz 3H). ^{13}C NMR (DMSO-d_6) δ 168.72, 167.58, 165.82, 163.95, 157.90, 135.54, 129.38, 129.03, 128.92, 128.21, 128.12, 127.94, 126.53, 126.41, 126.19, 110.94, 60.07, 32.12, 14.06; Mass (ESI, +ve) calculated for $[C_{17}H_{18}N_4O_5S]^+$ = 391.11, found 391.04.

Ethyl 2-(2-morpholinoethylthio)-6-oxo-1,6-dihydropyrimidine-5-carboxylate (41). A mixture of ethyl compound **39** (100 mg, 0.5 mmol), 4-(2-bromoethyl)morpholine (111 mg, 0.6 mmol) and potassium carbonate (207 mg, 1.5 mmol) in anhyd dimethyl formamide (3 mL) was stirred at rt for 16 h. The reaction was quenched with cold water (5 mL), extracted with ethyl acetate (3x10 mL). The combined organic layers were washed with brine (1x10 mL), dried over anhyd sodium sulfate, concentrated and the crude was purified by column chromatography (MeOH:CH_2Cl_2, 10:90) to obtain compound **41** as a white solid (94 mg, 60%). ^{1}H NMR (CD_3OD) δ 8.48 (s, 1H), 4.30 (q, J = 7.2 Hz, 2H), 3.94-3.86 (m, 4H), 3.39 (t, J = 6.3 Hz, 2H), 3.09 (t, J = 6.3 Hz, 2H), 2.94 (m, 4H), 1.34 (t, J = 7.2 Hz, 3H). ^{13}C NMR (CD_3OD) δ 66.47, 59.88, 54.16, 27.59, 14.56; Mass (ESI, +ve) calculated for $[C_{13}H_{20}N_3O_4S]^+$ = 314.12, found 314.13.

Ethyl 2-(2-morpholinoethylthio)-1-(2-oxo-2-phenylethyl)-pyrimidin-4-one-5-carboxylate (42). A mixture of **41** (100 mg, 0.31 mmol), 2-bromo-acetophenone (69 mg, 0.34 mmol) and potassium carbonate (43 mg, 0.31 mmol) in anhyd acetone (3 mL) was stirred at rt for 16 h. The reaction was quenched with cold water (5 mL), extracted with ethyl acetate (3 x 10 mL), combined organic layers were washed with brine (1x10 mL), dried over anhyd sodium sulfate, concentrated under reduced pressure and the crude compound was purified by column chromatography (5% MeOH:CH_2Cl_2) to obtain compound **42** as a white solid (89 mg, 65%). ^{1}H NMR (CD_3OD) δ 8.82 (s, 1H), 8.05 (d, J = 7.2

Hz, 2H), 7.70 (t, *J* = 7.2 Hz, 1H), 7.57 (t, *J* = 7.2 Hz, 2H), 5.91 (s, 2H), 4.38 (q, *J* = 7.1 Hz, 2H), 3.54 (m, 4H), 3.07 (m, 2H), 2.46 (m, 2H), 2.46 (m, 4H), 1.39 (t, *J* = 7.1 Hz, 3H). ^{13}C NMR (CD_3OD) δ 194.22, 176.64, 167.54, 164.56, 161.65, 135.57, 135.26, 130.15, 129.11, 108.62, 70.01, 67.60, 62.44, 58.49, 54.32, 28.77, 14.54; Mass (ESI, +ve) calculated for $[C_{21}H_{26}N_3O_5S]^+$ = 432.16, found 432.14.

2-(Morpholinomethyl)-6-oxo-3-phenyl-4,6-dihydropyrimido[2,1-b][1,3]thiazine-7-carboxylic acid (43). To a solution of compound **42** (100 mg, 0.23 mmol) in MeOH/ THF (1/3), LiOH (2.0 equiv) was added at rt, and was allowed to stir for 16 h. The reaction mixture was concentrated under reduced pressure, and water (5.0 mL) was added to the residue. The aqueous layer was acidified to pH 5 and the resulting precipitate was filtered, and washed with water (10.0 mL) to obtain compound **43** as a brown solid (36 mg, 40%). ^{1}H NMR (CD_3OD) δ 8.54 (s, 1H), 7.22 (m, 5H), 3.91 (m, 4H), 3.39 (m, 4H), 3.15 (t, *J* = 6.5 Hz, 2H), 2.70 (m, 2H). ^{13}C NMR (CD_3OD) δ 154.77, 137.07, 135.10, 134.50, 130.43, 129.74, 110.79, 65.07, 57.47, 53.55,25.62.

2-(2-Morpholinoethylthio)-*N*-(3-phenylpropyl)-pyrimidin-4-one-5-carboxamide (44). A stirred solution of trimethylaluminum (0.16 mL, 0.31 mmol, 2 M solution in toluene) in anhyd dichloromethane (5 mL) was treated with compound **41** (50 mg, 0.15 mmol) in anhyd dichloromethane (20 mL) at 0 °C. After stirring for 30 min, 3-phenylpropylamine (42 mg, 0.31 mmol) in anhyd dichloromethane (5 mL) was added and the mixture was stirred overnight at rt. The reaction mixture was then quenched with 0.1N sodium hydroxide solution at 0° C. The organic layer was washed with water (15 mL), brine (15 mL) and dried over anhyd Na_2SO_4. Combined organic layers were concentrated and the crude was purified by column chromatography (10% MeOH:CH_2Cl_2) to obtain compound **44** (38 mg, 60%) as a white solid. ^{1}H NMR (CD_3OD) δ 8.54 (s, 1H), 7.24 (m, 4H), 7.15 (t, *J* = 7.1 Hz, 1H), 3.89 (m, 4H), 3.38 (m, 4H), 3.12 (t, *J* = 6.5 Hz, 2H), 2.97 (m, 4H), 2.71 (m, 2H), 1.91 (m, 2H). ^{13}C NMR (CD_3OD) δ 170.23, 169.21, 167.02, 157.23, 142.80, 129.46, 129.45, 129.43, 126.93, 112.37, 66.40, 39.49, 34.15, 32.33, 27.62; Mass (ESI, +ve) calculated for

$[C_{20}H_{27}N_4O_3S]^+$ = 403.18, found 403.14.

Expression and purification of recombinant PfClpP protein. The recombinant PfClpP protein was obtained as described earlier (Rathore et al., 2010). Briefly, pET28a expression vector (Novagen) containing a fragment of *pfclpP* gene (168 aa–370 aa) which harbors the protease domain was transformed into *E. coli* expression cells BL21(DE3). These *E. coli* BL21(DE3) cells were grown in Luria broth containing kanamycin (25 mg/mL) and at 37 °C under shaking to an OD_{600} of 0.6 - 0.7 and expression of recombinant protein was induced with isopropyl-β-thioglactopyranoside (IPTG) at a final concentration of 1 mM. The cultures were further grown at 37°C for 3–4 h and the *E. coli* cells were harvested by centrifugation. The cell pellet was suspended in lysis buffer (50 mM Tris pH 8.0, 200 mM NaCl and 1% Tween-20) and the bacterial cells were lysed by sonication (Torebeo Ultrasonic Processor 36800, Cole-Parmer). The recombinant protein was purified from the lysate by affinity chromatography using Ni-nitrilotriaceticacid (Ni^{2+}-NTA) agarose resin (Qiagen), The eluates were analyzed on SDS-PAGE and the fractions containing the recombinant protein with a clear single band were pooled and the protein concentration was determined using the Pierce BCA (bicinchoninic acid) protein assay system and a standard curve of bovine serum albumin.

ClpP protease activity and inhibition assays: ClpP activity and its inhibition assays were carried out following Rathore et al.[8] Fluorimetric assays for the protease activities were carried out in 200 µl reaction volume containing 13 µM of recombinant protein in assay buffer (0.1 M sodium acetate pH 7.0, 1.0 mM DTT) in presence or absence of an inhibitor. The fluorogenic peptide substrate Suc-LLVY-AMC was added at 50 µM final concentration and the release of AMC was continuously monitored as the increase of fluorescence (excitation 355 nm; emission 460 nm) for 3-6 h at RT using a Victor-3 Fluorimeter (Perkin-Elmer). The IC_{50} values were calculated from curve fittings by software Workout V 2.5 and are shown in Table 1.

K_i was calculated from IC_{50} values using the equation: $K_i = \frac{IC50}{1+\left(\frac{[S]}{K_M}\right)}$, where the substrate concentration [S] is 50 μM and K_M = 34.3 μM.

Parasite culture and growth inhibition assays: P. falciparum strain 3D7 was cultured with 4% haematocrit in RPMI media (Invitrogen) supplemented with 0.5% albumax using a protocol described previously.[29] *P. falciparum* D10 ACP-GFP parasite lines were grown in same way and media was supplemented 100 nM pyrimethamine (Sigma). Parasite cultures were synchronized by repeated sorbitol treatment.[30] Parasite growth inhibition assays were carried out in 48-well plate as described earlier[8] and each assay was performed in triplicate and the experiment was repeated twice. Briefly, each well contained 0.5ml of complete media [RPMI (Invitrogen) with 0.5% albumax], 4% haematocrit and the parasitaemia adjusted to ~1%; the compound was added to the parasite cultures to desired final concentrations (0-100 μM) and same volume of solvent (DMSO) was added to the control wells. The cultures were allowed to grow further for 96 h. Parasite growth was assessed by DNA fluorescent dye-binding assay using SYBR green (Sigma) following Smilkstein et al.[31] For the apicoplast development assays, the ring stage (8-10 hpi) parasites (D10 ACP-GFP)[32] were treated with selected compounds. Parasites at different developmental stages (40 hpi and 72 hpi) were collected from the culture for fluorescence microscopy and stained with DAPI at a final concentration of 2 μg/mL for 30 min at 37 °C prior to imaging. The parasites were viewed using a Nikon A1R confocal laser-scanning microscope.

In vitro cell toxicity assay: Cytotoxicity assay was carried out by assessing the HeLa cells proliferation using MTT based calorimetric assay. HeLa cells were seeded in triplicates at 100 μL aliquots (1×103 cells per well) with DMEM medium in Nunclon flat bottom 96-well plates and were allowed to grow for 24 h. Subsequently, the medium was replaced by test medium containing each

inhibitor (0-5000 μM), or DMSO as control. The HeLa cells were allowed to grow for further 48 h, and then 10 μL of the MTT reagent was added and plates were incubated for 2 hrs. Remove the media and added 100 μL of DMSO to stop the reaction. The plates were read at 550 nm wavelengths using a microplate reader (Molecular Devices). The percentage growth was calculated by comparing with the control set.

Acknowledgement. Authors acknowledge the financial support from the Department of Biotechnology, Government of India, (grant #BT/IN/Canada/22/AM/2009 to A.M., P.M., and R.M.) and the Ministry of Research and Innovation, Government of Ontario (grant# CIISTDBTRD13-005 to LPK). The research in LPK laboratory is supported by the infrastructure fund from Canada Foundation for Innovation and Ontario Research Fund. The research work in AM's laboratory is supported by the Programme Support Grant (BT/01/CEIB/11/V/01) and Centre of Excellence grant (BT/COE/34/SP15138/2015) from the Department of Biotechnology, Govt. of India. MA is supported by research fellowship from ICMR, Govt. of India. SR is supported by INSA INSPIRE Faculty Fellowship from Department of Science and Technology, Govt. of India. We thank Rotary blood bank, New Delhi for providing the RBCs.

Supporting Information. ^{1}H NMR and HRMS data for the hit compounds **1-13** (commercial compounds); ^{1}H NMR, ^{13}C NMR, HPLC purity and melting points data for the synthesized compounds **22-44**.

References.

1. World Malaria Report 2015, World Health Organization.
2. Alonso, P. L.; Brown, G.; Arevalo-Herrera, M.; Binka, F.; Chitnis, C.; Collins, F.; Doumbo, O. K.; Greenwood, B.; Hall, B. F.; Levine, M. M.; et al. A Research Agenda to Underpin Malaria Eradication. *PLos Medicine* **2011**, *8*, e1000406. (doi:10.1371/journal.pmed.1000406)
3. Dondorp, A.; Nosten, F.; Yi, P.; Das, D.; Phyo, A.; Tarning, J.; Lwin, K.; Ariey, F.; Hanpithakpong, W.; Lee, S.; et al. Artemisinin resistance in *Plasmodium falciparum* malaria. *N. Engl. J. Med.* **2009**, *361*, 455-467.
4. Dhingra, N.; Jha, P.; Sharma, V.P.; Cohen, A.A.; Jotkar, R.M.; Rodriguez, P. S.; Bassani, D. G.; Suraweera, W.; Laxminarayan, R.; Peto, R. Adult and child malaria mortality in India: a nationally representative survey. *Lancet* **2010**, *376*, 1768-1774.
5. The malERA Consultative Group on Drugs. A research agenda for malaria eradication: Drugs. *PLoS Medicine* **2011**, *8*, e1000402. (doi:10.1371/journal.pmed.1000402)
6. De Mot, R.; Nagy, I.; Walz, J.; Baumeister, W. Proteasomes and other self compartmentalizing proteases in prokaryotes. *Trends Microbiol.* **1999**, *7(2)*, 88-92.
7. Ciechanover, A. Intracellular protein degradation: from a vague idea thru the lysosome and the ubiquitin-proteasome system and onto human diseases and drug targeting. *Cell Death Differ.* **2005**, *12(9)*, 1178-1190.
8. Rathore, S.; Sinha, D.; Asad, M.; Böttcher, T.; Afrin, F.; Chauhan, V.S.; Gupta, D.; Sieber, S.A.; Mohmmed A. A cyanobacterial serine protease of Plasmodium falciparum is targeted to the apicoplast and plays an important role in its growth and development. *Mol. Microbiol.* **2010**, *77(4)*, 873-890.
9. Ralph, S.A.; van Dooren, G.G.; Waller, R.F.; Crawford, M.J.; Fraunholz, M.J.; Foth, B.J.; Tonkin, C.J.; Roos, D.S.; McFadden, G.I. Tropical infectious diseases: metabolic maps and

functions of the *Plasmodium falciparum* apicoplast. *Nature Rev. Microbiol.* **2004**, *2(3)*, 203-216.

10. Williamson, D.H.; Preiser, P.R.; Moore, P.W.; McCready, S.; Strath, M.; Wilson, R.J. The plastid DNA of the malaria parasite *Plasmodium falciparum* is replicated by two mechanisms. *Mol. Microbiol.* **2002**, *45(2)*, 533-542.
11. McConkey, G.A.; Rogers, M.J.; McCutchan, T.F. Inhibition of *Plasmodium falciparum* protein synthesis. Targeting the plastid-like organelle with thiostrepton. *J. Biol. Chem.* **1997**, *272(4)*, 2046-2049.
12. Lin, Q.; Katakura, K.; Suzuki, M. Inhibition of mitochondrial and plastid activity of *Plasmodium falciparum* by minocycline. *FEBS Lett.* **2002**, *515(1-3)*, 71-74.
13. Chaubey, S.; Kumar, A.; Singh, D.; Habib, S. The apicoplast of *Plasmodium falciparum* is translationally active. *Mol. Microbiol.* **2005**, *56(1)*, 81-89.
14. El Bakkouri, M.; Rathore, S.; Calmettes, C.; Wernimont, A.K.; Liu, K.; Sinha, D.; Asad, M.; Jung, P.; Hui, R.; Mohmmed, A.; Houry, W. A. Structural insights into the inactive subunit of the apicoplast-localized caseinolytic protease complex of *Plasmodium falciparum*. *J. Biol. Chem*. **2013**, *288(2)*, 1022-1031.
15. Vedadi, M.; Lew, J.; Artz, J.; Amani, M.; Zhao, Y.; Dong, A.; Wasney, G.A.; Gao, M.; Hills, T.; Brokx, S.; et al. Genome-scale protein expression and structural biology of *Plasmodium falciparum* and related Apicomplexan organisms. *Mol. Biochem. Parasitol.* **2007**, *151*, 100-110.
16. Szyk, A.; Maurizi, M. R. Crystal structure at 1.9A of E. coli ClpP with a peptide covalently bound at the active site. *J. Struct. Biol.* **2006**, *156*, 165-174.
17. Dahl, E.L.; Rosenthal, P.J. Multiple antibiotics exert delayed effects against the Plasmodium falciparum apicoplast. *Antimicrob Agents Chemother.* **2007**, *51(10)*, 3485-90.

18. Goodman, C.D.; Pasaje; C.F.; Kennedy, K.; McFadden, G.I.; Ralph, S.A. Targeting Protein Translation in Organelles of the Apicomplexa. *Trends Parasitol.* **2016**, *32(12)*, 953-965.

19. Blackman, M. J. Proteases involved in erythrocyte invasion by the malaria parasite: function and potential as chemotherapeutic targets. *Curr. Drug Targets* **2000**, *1(1)*, 59-83.

20. Rosenthal, P. J. Hydrolysis of erythrocyte proteins by proteases of malaria parasites. *Curr. Opin. Hematol.* **2002**, *9(2)*, 140-145.

21. Goodman, C.D.; Su, V.; McFadden, G.I. The effects of anti-bacterials on the malaria parasite Plasmodium falciparum. *Mol. Biochem. Parasitol.* **2007**, *152(2)*,181-191.

22. Pradel, G.; Schlitzer, M. Antibiotics in malaria therapy and their effect on the parasite apicoplast. *Curr. Mol. Med.* **2010**, *10(3)*, 335-349.

23. Dahl, E.L.; Rosenthal, P. J. Apicoplast translation, transcription and genome replication: targets for antimalarial antibiotics. *Trends Parasitol.* **2008**, *24(6)*, 279-284.

24. Fleige, T.; Soldati-Favre, D. Targeting the transcriptional and translational machinery of the endosymbiotic organelle in apicomplexans. *Curr. Drug Targets* **2008**, *9(11)*, 948-956.

25. Barthel, D.; Schlitzer, M.; Pradel, G. Telithromycin and quinupristin-dalfopristin induce delayed death in Plasmodium falciparum. *Antimicrob. Agents Chemother.* **2008**, *52(2)*, 774-777.

26. Ekland, E.H.; Schneider, J.; Fidock, D.A. Identifying apicoplast-targeting antimalarials using high-throughput compatible approaches. *FASEB J.* **2011**, *25(10)*, 3583-3593.

27. Goodman, C.D.; McFadden, G.I. Targeting apicoplasts in malaria parasites. *Expert Opin. Ther. Targets* **2013**, *17(2)*, 167-177.

28. Case, D.A.; Darden, T.A.; Cheatham, III, T.E.; Simmerling, C.L.; Wang, J.; Duke, R. E.; Luo, R.; Walker, R. C.; Zhang, W.; Merz, K. M.; et al. AMBER 11, **2010**, University of California, San Francisco.

29. Trager, W.; Jensen, J. B. Human malaria parasites in continuous culture. *Science* **1976**, *193(4254)*, 673-675.

30. Lambros, C.; Vanderberg, J. P. Synchronization of Plasmodium falciparum erythrocytic stages in culture. *J. Parasitol.* **1979**, *65(3)*, 418-420.

31. Smilkstein, M.; Sriwilaijaroen, N.; Kelly, J.X.; Wilairat, P.; Riscoe, M. Simple and inexpensive fluorescence-based technique for high-throughput antimalarial drug screening. *Antimicrob. Agents Chemother.* **2004**, *48(5)*, 1803-1806.

32. Waller, R.F.; Reed, M.B.; Cowman, A.F.; McFadden, G.I. Protein trafficking to the plastid of *Plasmodium falciparum* is via the secretory pathway. *EMBO J.* **2000**, *19(8)*, 1794-1802.

TOC Graphic.

A novel class of *Plasmodial* ClpP protease inhibitors as potential antimalarial agents.

S. Mundra, V. Thakur, A.M. Bello, S. Rathore, M. Asad, L. Wei, J. Yang, S. K. Chakka, R. Mahesh, P. Malhotra, A. Mohmmed,* L.P. Kotra.*